J Fourier Anal Appl (2018) 24:872–907
https://doi.org/10.1007/s00041-017-9540-z

Directional Wavelet Bases Constructions with Dyadic Quincunx Subsampling

Rujie Yin[1] · **Ingrid Daubechies**[1]

Received: 5 October 2016 / Revised: 22 February 2017 / Published online: 13 April 2017

Abstract We construct directional wavelet systems that will enable building efficient signal representation schemes with good direction selectivity. In particular, we focus on wavelet bases with dyadic quincunx subsampling. In our previous work (Yin, in: Proceedings of the 2015 international conference on sampling theory and applications (SampTA), 2015), we show that the supports of orthonormal wavelets in our framework are discontinuous in the frequency domain, yet this irregularity constraint can be avoided in frames, even with redundancy factor <2. In this paper, we focus on the extension of orthonormal wavelets to biorthogonal wavelets and show that the same obstruction of regularity as in orthonormal schemes exists in biorthogonal schemes. In addition, we provide a numerical algorithm for biorthogonal wavelets construction where the dual wavelets can be optimized, though at the cost of deteriorating the primal wavelets due to the intrinsic irregularity of biorthogonal schemes.

Keywords MRA · Directional wavelet bases · Perfect reconstruction · Dyadic quincunx downsampling · Optimization

Mathematics Subject Classification 42C40

Communicated by Gitta Kutyniok.

✉ Rujie Yin
rujie.yin@duke.edu

Ingrid Daubechies
ingrid@math.duke.edu

1 Department of Mathematics, Duke University, Durham, NC, USA

1 Introduction

In image compression and analysis, 2D tensor wavelet schemes are widely used. Despite the time-frequency localization inherited from 1D wavelet, 2D tensor wavelets suffer from poor orientation selectivity: only horizontal or vertical edges are well represented by tensor wavelets. To obtain better representation of 2D images, several directional wavelet schemes have been proposed and applied to image processing, such as directional wavelet filterbanks (DFB) and various extensions.

Conventional DFB [1] divides the square frequency domain associated with a regular 2D lattice into eight equi-angular pairs of triangles; such schemes can be critically downsampled (maximally decimated) with perfect reconstruction (PR), but they typically do not have a multi-resolution structure. Different approaches have been proposed to generalize DFB to multi-resolution systems, including non-uniform DFB (nuDFB), contourlets, curvelets, shearlets and dual-tree wavelets. nuDFB is introduced in [13] based on multi-resolution analysis (MRA), where at each level of decomposition the square frequency domain is divided into a high frequency outer ring and a central low frequency domain. For nuDFB, the high frequency ring is primarily divided further into six equi-angular pairs of trapezoids and the central low frequency square is kept intact for division in the next level of decomposition, see the left panel in Fig. 1. The nuDFB filters are solved by optimization which provides non-unique near orthogonal or bi-orthogonal solutions depending on the initialization without stable convergence. Contourlets [6] combine the Laplacian pyramid scheme with DFB which has PR but with redundancy $4/3$ inherited from the Laplacian pyramid. Shearlet [9,14] and curvelet [3] systems construct a multi-resolution partition of the frequency domain by applying shear or rotation operators to a generator function in each level of frequency decomposition. These systems have redundancy at least 4; moreover, the factor may grow with the number of directions in the decomposition level.[1] In numerical implentations of shearlets, the redundancy rate can be reduced to 2.6 using specific numerical techniques to enforce perfect reconstruction when decreasing the sampling rate [10]. In general, shearlets can be viewed as a particular example of composite dilation wavelets (CDW), where aside from the normal translations on a lattice, a group of matrices in $SL(d, \mathbb{R})$, e.g. shear matrices in the case of shearlets, is also used as "shifts", see [2] for a general framework of CDW and composite MRA.[2] Despite non-separable constructions, better direction specification of 2D tensor wavelets can be achieved by their linear combinations. For example, dual-tree wavelets [15] are linear combinations of 2D tensor wavelets (corresponding to multi-resolution systems) that constitute an approximate Hilbert transform pair, where the high frequency ring is divided into pairs of squares of different directional preference. More general directional tensor product complex tight framelets in d-dimension have been constructed in [11] with a redundancy rate of $\frac{3^d-1}{2^d-1}$.

None of these multi-resolution schemes is PR, critically downsampled and regularized (localized in both time and frequency). In the framework of nuDFB ([13]), it

1 Online packages are available at CurveLab http://www.curvelet.org/ and ShearLab http://www.shearlab.org/.

2 Several critically sampled CDW schemes are proposed in [8].

was shown by Durand [7] that it is impossible to construct orthonormal filters localize without discontinuity in the frequency domain, or—equivalently—regularized filters without aliasing. His construction of directional filters uses compositions of 2-band filters associated to quincunx lattice, similar to that of uniform DFB in [13]; as pointed out in [13] the overall composed filters are not alias-free. It is not clear whether Durand's argument also precludes the existence of a regularized wavelet system, if one slightly weakens the set of conditions.

To study this question, we consider multi-resolution directional wavelets corresponding to the same partition of frequency domain as nuDFB and build a framework to analyze the equivalent conditions of PR for critically downsampled as well as more general redundant schemes. In our previous work [16], we show that in MRA on a dyadic quincunx lattice, PR is equivalent to an identity condition and a set of shift-cancellation conditions closely related to the frequency support of filters and their downsampling scheme. Based on these two conditions, we rederived Durand's discontinuity result of orthonormal schemes; we also show that a slight relaxation of conditions allows frames with redundancy <2 that circumvent the regularity limitation. Furthermore, we have an explicit approach to construct such regularized directional wavelet frames by smoothing the Fourier transform of the irregular directional wavelets. The main contribution of this paper is that we extend our previous work and show that the same obstruction to regularity as in orthonormal schemes exists in biorthogonal schemes. Different from our previous approach in the orthonormal case, our analysis of bi-orthogonal schemes is inspired by Cohen et al's approach in [5] for numerical construction of compactly supported symmetric wavelet bases on a hexagonal lattice. We extend and adapt their numerical construction to our bi-orthogonal setting.

The paper is organized as follows. In Sect. 2, we set up the framework of an MRA with dyadic quincunx downsampling. In Sect. 3, we review the regularity analysis of orthonormal schemes and its extension to frames in [16]. In particular, we derive two conditions, *identity summation* and *shift cancellation*, equivalent to perfect reconstruction in this MRA with critical downsampling. These lead to the classification of *regular/singular* boundaries of the frequency partition and a *relaxed shift-cancellation* condition for low-redundancy MRA frame allows better regularity of the directional wavelets. In Sect. 4, we extend the orthonormal schemes to biorthogonal schemes as well as the corresponding *identity summation* and *shift cancellation* conditions. We then introduce Cohen et al's approach in [5] and adapt it to the regularity analysis on our biorthogonal schemes due to these conditions. We show that the biorthogonal schemes have the same irregularity as in the orthonormal schemes. In Sect. 5, we propose a numerical algorithm for the construction of biorthogonal schemes along with further analysis on the regularity constraints. Finally, we present and discuss numerical results of our algorithm in Sect. 6, and conclude our current work in Sect. 7.

2 Framework Setup

We summarize 2D-MRA systems and the relation between frequency domain partition and sublattice of $\mathbb{Z}^2$ with critical downsampling following [16].

2.1 Notations and Conventions

Throughout this paper, we use upper case bold font for matrices (e.g. $\boldsymbol{A}$, $\boldsymbol{B}$), lower case bold font for vectors (e.g. $\boldsymbol{a}$, $\boldsymbol{b}$) and upper case italics for subsets (e.g. C_1, C_2) of the frequency domain. We denote the conjugate transpose of a matrix $\boldsymbol{A}$ by $\boldsymbol{A}^*$. For $\boldsymbol{a}$ in a d-dimensional vector space over $\mathbb{F}$, we use the convention $\boldsymbol{a} \in \mathbb{F}^{d\times 1}$ and $\boldsymbol{a}^*$ for its conjugate row vector.

We adopt conventions in scientific computing programs and packages. For matrices and vectors, the indexing of rows and columns starts with zero. For the axes of the frequency plane, we denote the vertical axis as ω_1-axis with values increasing from top to bottom and the horizontal axis as ω_2-axis with values increasing from left to right, e.g. Fig. 1.

2.2 Multi-resolution Analysis and Sublattice Sampling

In an MRA, given a scaling function $\phi \in L^2(\mathbb{R}^2)$, such that $\|\phi\|_2 = 1$, the base approximation space is defined as $V_0 = \overline{span\{\phi_{0,\boldsymbol{k}}\}_{\boldsymbol{k}\in\mathbb{Z}^2}}$, where $\phi_{0,\boldsymbol{k}} = \phi(\boldsymbol{x} - \boldsymbol{k})$. If $\langle\phi_{0,\boldsymbol{k}}, \phi_{0,\boldsymbol{k}'}\rangle = \delta_{\boldsymbol{k},\boldsymbol{k}'}$, then $\{\phi_{0,\boldsymbol{k}}\}$ is an orthonormal basis of V_0. In addition, ϕ is associated with a scaling matrix $\mathbf{D} \in \mathbb{Z}^{2\times 2}$, such that the dilated scaling function $\phi_1(\boldsymbol{x}) = |\mathbf{D}|^{-1/2}\phi(\mathbf{D}^{-1}\boldsymbol{x})$ is a linear combination of $\phi_{0,\boldsymbol{k}}$. Equivalently, $\exists\, m_0(\boldsymbol{\omega}) = m_0(\omega_1, \omega_2)$, $2\pi-$periodic in ω_1, ω_2, s.t. in the frequency domain

$$\widehat{\phi}\left(\mathbf{D}^T\boldsymbol{\omega}\right) = m_0(\boldsymbol{\omega})\widehat{\phi}(\boldsymbol{\omega}). \tag{1}$$

The recursive expression (1) of $\widehat{\phi}(\boldsymbol{\omega})$ implies that

$$\widehat{\phi}(\boldsymbol{\omega}) = (2\pi)^{-1}\prod_{k=1}^{\infty} m_0\big(\mathbf{D}^{-k}\boldsymbol{\omega}\big), \tag{2}$$

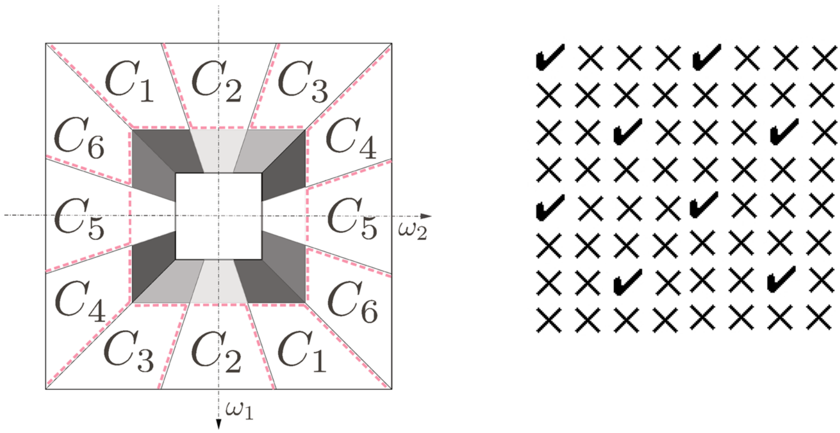

Fig. 1 *Left* partition of S_0 and boundary assignment of C_j, $j = 1, \ldots, 6$ (each C_j has boundaries indicated by *red dashed line segments*), *Right* dyadic quincunx sublattice. Note that the ω_1-axis is vertical and the ω_2-axis is horizontal by our convention (Color figure online)

where we have implicitly assumed that $\phi \in L^1(\mathbb{R}^2)$ and $\int \phi\, dx = 1$ (which follows from the other constraints if ϕ has some decay at ∞).

Let $\phi_{l,\boldsymbol{k}} = \phi(\boldsymbol{D}^{-l}\boldsymbol{x} - \boldsymbol{k})$ and $V_l = \overline{span\{\phi_{l,\boldsymbol{k}}; \boldsymbol{k} \in \mathbb{Z}^2\}}$, $l \in \mathbb{Z}$ be the nested approximation spaces. Define W_l as the orthogonal complement of V_l with respect to V_{l-1} in MRA. Suppose there are J wavelet functions $\psi^j \in L^2(\mathbb{R}^2)$, $1 \le j \le J$, and $\mathbf{Q} \in \mathbb{Z}^{2\times 2}$, s.t.

$$W_l = \bigcup_{j=1}^{J} W_l^j = \bigcup_{j=1}^{J} \overline{span\{\psi_{l,\boldsymbol{k}}^j; \boldsymbol{k} \in \mathbf{Q}\mathbb{Z}^2\}} = \bigcup_{j=1}^{J} \overline{span\{\psi^j(\mathbf{D}^{-l}\boldsymbol{x} - \boldsymbol{k}); \boldsymbol{k} \in \mathbf{Q}\mathbb{Z}^2\}},$$

an L-level multi-resolution system with base space V_0 is then spanned by

$$V_L \oplus \bigoplus_{l=1}^{L} \left(\bigcup_{j=1}^{J} W_l^j \right) = \{\phi_{L,\boldsymbol{k}}, \psi_{l,\boldsymbol{k}'}^j,\ 1 \le l \le L,\ \boldsymbol{k} \in \mathbb{Z}^2,\ \boldsymbol{k}' \in \mathbf{Q}\mathbb{Z}^2,\ 1 \le j \le J\}. \tag{3}$$

As $W_1 \subset V_0$, each rescaled wavelet $\psi^j(\mathbf{D}^{-1}\cdot)$ is also a linear combination of $\phi_{0,\boldsymbol{k}}$, so that there exists m_j analogous to m_0 satisfying

$$\widehat{\psi}^j\left(\mathbf{D}^T\boldsymbol{\omega}\right) = m_j(\boldsymbol{\omega})\widehat{\phi}(\boldsymbol{\omega}), \qquad 1 \le j \le J. \tag{4}$$

2.3 Frequency Domain Partition and Critical Downsampling

Consider the canonical frequency square, $S_0 = [-\pi, \pi) \times [-\pi, \pi)$ associated with the lattice $\mathcal{L} = \mathbb{Z}^2$. For $L = 1$, the 1-level decomposition (3) together with (1) and (4) implies that the union of the support of m_j, $0 \le j \le J$ covers S_0. Furthermore, there exist $C_j \subset supp(m_j), 0 \le j \le J$, such that they form a partition of S_0; conversely, given a partition C_j of S_0, we may construct an MRA where m_j are "mainly" supported on C_j (this will become more explicit in Sect. 4.3). To build an orthonormal basis with good directional selectivity, we choose the partition of S_0 shown in the left of Fig. 1, which is the same for Example B in [7], or equivalently the frequency partition in the coarsest level of the least redundant shearlet system [12]. In this partition, S_0 is divided into a central square $C_0 = \begin{pmatrix} 2 & 0 \\ 0 & 2 \end{pmatrix}^{-1} S_0$ and a ring: the ring is further cut into six pairs of directional trapezoids C_j by lines passing through the origin with slopes ± 1, ± 3 and $\pm\frac{1}{3}$. The central square C_0 can be further partitioned in the same way to obtain a two-level multi-resolution system, as shown in Fig. 1.

In the corresponding MRA generated by (3), $J = 6$ and $\mathbf{D} = \begin{pmatrix} 2 & 0 \\ 0 & 2 \end{pmatrix}$, and we choose $\mathbf{Q}$ specifically to be $\begin{pmatrix} 1 & 1 \\ -1 & 1 \end{pmatrix}$. Because $|\mathbf{D}|^{-1} + J|\mathbf{QD}|^{-1} = 1/4 + 6/(2 \cdot 4) = 1$, the corresponding MRA generated by (3) achieves critical downsampling([7]). The scaling matrix of ψ^j is $\boldsymbol{QD} = \begin{pmatrix} 2 & 2 \\ -2 & 2 \end{pmatrix}$, which corresponds to downsampling on the dyadic quincunx sublattice $\boldsymbol{QD}\mathbb{Z}^2$ (see the right panel in Fig. 1), as in [7].

This downsampling scheme is compatible with C_j. Consider two sets of shifts in the frequency domain $\Gamma_0 = \{\boldsymbol{\pi}_i,\ i = 0, 2, 4, 6\}$ and $\Gamma_1 = \{\boldsymbol{\pi}_i,\ i = 0, 1, \ldots, 7\}$, where $\boldsymbol{\pi}_0 = (0, 0), \boldsymbol{\pi}_1 = (\pi/2, \pi/2), \boldsymbol{\pi}_2 = (\pi, 0), \boldsymbol{\pi}_3 = (-\pi/2, \pi/2),\ \boldsymbol{\pi}_4 = (0, \pi), \boldsymbol{\pi}_5 = (\pi/2, -\pi/2), \boldsymbol{\pi}_6 = (\pi, \pi), \boldsymbol{\pi}_7 = (-\pi/2, -\pi/2)$. Γ_0 and Γ_1 characterize the sublattices $\boldsymbol{D}\mathbb{Z}^2$ and $\boldsymbol{QD}\mathbb{Z}^2$ respectively by $\sum_{\boldsymbol{\pi}\in\Gamma_0} e^{i\boldsymbol{\alpha}^\top\boldsymbol{\pi}} = |\Gamma_0|\, \mathbb{1}_{\boldsymbol{D}\mathbb{Z}^2}(\boldsymbol{\alpha})$ and $\sum_{\boldsymbol{\pi}\in\Gamma_1} e^{i\boldsymbol{\alpha}^\top\boldsymbol{\pi}} = |\Gamma_1|\, \mathbb{1}_{\boldsymbol{QD}\mathbb{Z}^2}(\boldsymbol{\alpha})$, where $\mathbb{1}$ is the indicator function. We observe that each C_j forms a tiling of S_0 under the shifts associated with the sublattice where the coefficients of ψ^j are downsampled:

$$S_0 = \bigcup_{\boldsymbol{\pi}\in\Gamma_1} \left(C_j + \boldsymbol{\pi}\right) = \bigcup_{\boldsymbol{\pi}\in\Gamma_0} (C_0 + \boldsymbol{\pi}), \quad j = 1, \ldots, 6. \tag{5}$$

Alternatively, we say that $\{\,C_j,\ j = 0, \ldots, 6\,\}$ is an *admissible* partition of S_0 with respect to the dyadic quincunx downsampling scheme. The admissible property guarantees the existence of orthonormal bases consisting of directional filters on the dyadic quincunx sublattice with frequency support in C_j.

3 Orthonormal Bases

In this section, we discuss the conditions on m_j such that the corresponding MRA forms an orthonormal bases.

We begin with the two key conditions, i.e. *identity summation* and *shift cancellation*, on m_j such that the system (3) is perfect-reconstruction (PR) or equivalently a Parseval frame in MRA.

3.1 Orthonormal Conditions on m_j

In MRA, (3) is PR if for all $f \in L_2(\mathbb{R}^2)$,

$$\sum_{\boldsymbol{k}\in\mathbb{Z}^2} \langle f, \phi_{0,\boldsymbol{k}}\rangle \phi_{0,\boldsymbol{k}} = \sum_{\boldsymbol{k}\in\mathbb{Z}^2} \langle f, \phi_{1,\boldsymbol{k}}\rangle \phi_{1,\boldsymbol{k}} + \sum_{j=1}^{J} \sum_{\boldsymbol{k}'\in \boldsymbol{Q}\mathbb{Z}^2} \langle f, \psi^j_{1,\boldsymbol{k}'}\rangle \psi^j_{1,\boldsymbol{k}'}. \tag{6}$$

Using (1) and (4) together with the admissibility of the frequency partition (5), condition (6) on ϕ and ψ^j yields:

Theorem 1 *Let* $J = 6$, $\boldsymbol{D} = \begin{pmatrix} 2 & 0 \\ 0 & 2 \end{pmatrix}$ *and* $\boldsymbol{Q} = \begin{pmatrix} 1 & 1 \\ -1 & 1 \end{pmatrix}$ *in* (3)*. Then the perfect reconstruction condition holds for* (3) *if and only if the following two conditions hold.*

$$|m_0(\boldsymbol{\omega})|^2 + \sum_{j=1}^{6} |m_j(\boldsymbol{\omega})|^2 = 1. \tag{7}$$

$$\begin{cases} \sum_{j=0}^{6} m_j(\boldsymbol{\omega})\overline{m_j}(\boldsymbol{\omega}+\boldsymbol{\pi}) = 0, & \boldsymbol{\pi} \in \Gamma_0 \backslash \{\mathbf{0}\}. \\ \sum_{j=1}^{6} m_j(\boldsymbol{\omega})\overline{m_j}(\boldsymbol{\omega}+\boldsymbol{\pi}) = 0, & \boldsymbol{\pi} \in \Gamma_1 \backslash \Gamma_0. \end{cases} \tag{8}$$

Theorem 1 is a corollary of Proposition 1 and Proposition 2 in [7]. We give an alternate proof in Appendix 1. In Theorem 1, (7) is the *identity summation* condition, guaranteeing conservation of l_2 energy; (8) is the *shift cancellation* condition such that aliasing is canceled correctly in reconstruction from wavelet coefficients. Because each m_j is $(2\pi, 2\pi)$ periodic, we only need to check these conditions for $\boldsymbol{\omega} \in S_0$.

Moreover, for (3) to be an orthonormal basis, $\{\phi_{\boldsymbol{k}}\}_{\boldsymbol{k}\in\mathbb{Z}^2}$ need to be an orthonormal basis, which is determined by m_0 in (2). In 1D MRA, Cohen's theorem in [4] provides a necessary and sufficient condition on m_0 such that (3) is an orthonormal basis. This theorem generalizes to 2D in e.g. [16], as follows.

Theorem 2 *Assume that* m_0 *is a trigonometric polynomial with* $m_0(\mathbf{0}) = 1$*, and define* $\hat{\phi}(\boldsymbol{\omega})$ *as in* (2).

If $\phi(\cdot - \boldsymbol{k}), \boldsymbol{k} \in \mathbb{Z}^2$ *are orthonormal, then there exists* K *containing a neighborhood of 0, such that for any* $\boldsymbol{\omega} \in S_0$, $\boldsymbol{\omega} + 2\pi\mathbf{n} \in K$ *for some* $\mathbf{n} \in \mathbb{Z}^2$*, and* $\inf_{k>0,\, \boldsymbol{\omega}\in K} |m_0(\mathbf{D_2}^{-k}\boldsymbol{\omega})| > 0$*. Further, if* $\sum_{\boldsymbol{\pi}\in\Gamma_0} |m_0(\boldsymbol{\omega}+\boldsymbol{\pi})|^2 = 1$*, then the inverse is true.*

3.2 Regularity of m_j Supported on the C_j

In this subsection, we consider m_j supported on the C_j introduced in Sect. 2.3 that satisfy orthonormal conditions in Sect. 3.1. We begin with the Shannon-type wavelet construction, where m_j are indicator functions $m_j = \mathbb{1}_{C_j}$, $0 \le j \le 6$, and we use the boundary assignment of C_j in Fig. 1. The identity summation follows from the partition of S_0 by the C_j, and the shift cancellation follows from the admissible property (5). Applying Theorem 2 to m_0, we verify that the Shannon-type wavelets generated from these m_j form an orthonormal basis.

Because of the discontinuity at ∂C_j, the boundaries of the C_j, these m_j are not smooth, and hence the corresponding wavelets are not spatially localized. The m_j can be regularized by smoothing at the ∂C_j. However, as shown in Proposition 3 in [7], it is not possible to smooth the behavior of the m_j at *all* the boundaries with discontinuity if the m_j have to satisfy the perfect reconstruction condition. In [16], the ∂C_j are segmented into *singular* and *regular* pieces with respect to the shift cancellation condition (8) in Theorem 1. On regular boundaries, pairs of $(m_j, m_{j'})$ share a boundary and can both be smoothed in a coherent way such that both (7) and (8) remain satisfied. The singular pieces are boundaries for just one m_j, which can then not be smoothed without violating the shift cancellation condition. Figure 2 shows the boundary classification, where the corners of S_0 and C_0 are singular, hence m_0 and the m_j's in two diagonal directions of an orthonormal bases are discontinuous there.

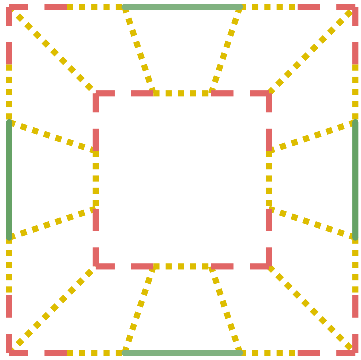

Fig. 2 Boundary classification: singular (*red dashed*) and regular (*yellow dotted*). The *green solid lines* are continuous segments due to periodicity (Color figure online)

A mechanism of constructing orthonormal bases by smoothing Shannon-type m_j on regular boundaries is provided in [16].

3.3 Extension to Low-Redundancy Tight Frame

The irregularity of orthonormal bases can be overcome in the following low-redundancy tight frame construction,

$$\{\phi_{L,\boldsymbol{k}}, \psi^j_{l,\boldsymbol{k}'}, 1 \le l \le L, \boldsymbol{k}, \boldsymbol{k}' \in \mathbb{Z}^2, 1 \le j \le 6\}. \tag{9}$$

In (9), all wavelet coefficients are downsampled on the dyadic sublattice and the redundancy of any such $L-$level frame does not exceed $\frac{J/|D|}{1-1/|D|} = \frac{6/4}{1-1/4} = 2$. Similar to Theorem 1, we have

Theorem 3 *Equation* (9) *has PR if and only if the following two conditions both hold.*

$$|m_0(\boldsymbol{\omega})|^2 + \sum_{j=1}^{6} |m_j(\boldsymbol{\omega})|^2 = 1. \tag{10}$$

$$\sum_{j=0}^{6} m_j(\boldsymbol{\omega})\overline{m_j}(\boldsymbol{\omega} + \boldsymbol{\pi}) = 0, \quad \boldsymbol{\pi} \in \Gamma_0 \backslash \{\boldsymbol{0}\}. \tag{11}$$

Theorem 3 can be proved analogously to Theorem 1, but with fewer shift cancellation constraints. Following the same analysis of boundary regularity as before, we show in [16] that all boundaries are regular with respect to (10) and can be smoothed properly. Hence, we were able to obtain directional wavelets with much better spatial and frequency localization than those constructed by Durand in [7].

So far, we have considered two directional wavelet MRA systems (3) and (9) such that the directional wavelets characterize 2D signals in six equi-angled directions. Furthermore, these wavelets are well localized in the frequency domain. In particular, for a fixed small $\epsilon > 0$, we can construct m_j such that $supp(m_j)$ is convex and

$$\sup_{\boldsymbol{\omega}' \in supp(m_j) \cap S_0} \inf_{\boldsymbol{\omega} \in C_j} \|\boldsymbol{\omega}' - \boldsymbol{\omega}\| < \epsilon, \quad 0 \leq j \leq 6. \tag{12}$$

This desirable condition is hard to obtain by multi-directional filter bank assembly of several elementary filter banks.

In the next section, we analyze the more general case of directional bi-orthorgonal filters constructed with respect to the same frequency partition.

4 Biorthogonal Bases

In this section, we analyze biorthogonal bases in the following form of MRA,

$$\{\phi_{L,\boldsymbol{k}}, \widetilde{\phi}_{L,\boldsymbol{k}}, \psi^j_{l,\boldsymbol{k}'}, \widetilde{\psi}^j_{l,\boldsymbol{k}'}, \quad 1 \leq l \leq L, \ \boldsymbol{k} \in \mathbb{Z}^2, \quad \boldsymbol{k}' \in \mathbf{Q}\mathbb{Z}^2, \ 1 \leq j \leq 6\}, \tag{13}$$

where ϕ and ψ^j satisfy (1) and (4) respectively, and likewise for $\widetilde{\phi}$ and $\widetilde{\psi^j}$,

$$\widehat{\widetilde{\phi}}(\boldsymbol{D}^T\boldsymbol{\omega}) = \widetilde{m_0}(\boldsymbol{\omega})\widehat{\widetilde{\phi}}(\boldsymbol{\omega}), \quad \widehat{\widetilde{\psi^j}}(\boldsymbol{D}^T\boldsymbol{\omega}) = \widetilde{m_j}(\boldsymbol{\omega})\widehat{\widetilde{\phi}}(\boldsymbol{\omega}). \tag{14}$$

For such biorthogonal bases, we have the similar identity summation and shift cancellation conditions to those in Theorem 1.

Theorem 4 *Equation* (13) *has PR if and only if the following two conditions hold*

$$m_0(\boldsymbol{\omega})\overline{\widetilde{m_0}}(\boldsymbol{\omega}) + \sum_{j=1}^{6} m_j(\boldsymbol{\omega})\overline{\widetilde{m_j}}(\boldsymbol{\omega}) = 1, \tag{15}$$

$$\begin{cases} \sum\limits_{j=0}^{6} m_j(\boldsymbol{\omega})\overline{\widetilde{m_j}}(\boldsymbol{\omega}+\boldsymbol{\pi}) = 0, & \boldsymbol{\pi} \in \Gamma_0\backslash\{\mathbf{0}\}. \\ \sum\limits_{j=1}^{6} m_j(\boldsymbol{\omega})\overline{\widetilde{m_j}}(\boldsymbol{\omega}+\boldsymbol{\pi}) = 0, & \boldsymbol{\pi} \in \Gamma_1\backslash\Gamma_0. \end{cases} \tag{16}$$

We also have the following analogue of Theorem 2.

Theorem 5 *Assume that $m_0, \widetilde{m_0}$ are trigonometric polynomials with $m_0(\mathbf{0}) = \widetilde{m_0}(\mathbf{0}) = 1$, which generate $\phi, \widetilde{\phi}$ respectively.*

If $\phi(\cdot - \boldsymbol{k}), \widetilde{\phi}(\cdot - \boldsymbol{k})$, $\boldsymbol{k} \in \mathbb{Z}^2$ are biorthogonal, then there exists K containing a neighborhood of 0, such that for any $\boldsymbol{\omega} \in S_0$, $\boldsymbol{\omega} + 2\pi\mathbf{n} \in K$ for some $\mathbf{n} \in \mathbb{Z}^2$, and $\inf_{k>0,\, \boldsymbol{\omega}\in K} |m_0(\mathbf{D_2}^{-k}\boldsymbol{\omega})| > 0$, $\inf_{k>0,\, \boldsymbol{\omega}\in K} |\widetilde{m_0}(\mathbf{D_2}^{-k}\boldsymbol{\omega})| > 0$. Furthermore, if $\sum_{\boldsymbol{\pi}\in\Gamma_0} m_0(\boldsymbol{\omega}+\boldsymbol{\pi})\overline{\widetilde{m_0}}(\boldsymbol{\omega}+\boldsymbol{\pi}) = 1$, then the inverse is true.

By Theorem 5, m_0 and $\widetilde{m_0}$ need to satisfy the following identity constraint for the MRA (13) to be biorthogonal,

$$m_0\overline{\widetilde{m_0}}(\boldsymbol{\omega}) + m_0\overline{\widetilde{m_0}}(\boldsymbol{\omega}+\boldsymbol{\pi}_2) + m_0\overline{\widetilde{m_0}}(\boldsymbol{\omega}+\boldsymbol{\pi}_4) + m_0\overline{\widetilde{m_0}}(\boldsymbol{\omega}+\boldsymbol{\pi}_6) = 1. \tag{17}$$

Furthermore, the identity summation and shift cancellation conditions (15) and (16) from Theorem 4 can be combined into a linear system with respect to m_j as follows,

$$\begin{bmatrix} \overline{\widetilde{m_0}}(\boldsymbol{\omega}) & \overline{\widetilde{m_1}}(\boldsymbol{\omega}) & \dots & \overline{\widetilde{m_6}}(\boldsymbol{\omega}) \\ 0 & \overline{\widetilde{m_1}}(\boldsymbol{\omega}+\boldsymbol{\pi}_1) & \dots & \overline{\widetilde{m_6}}(\boldsymbol{\omega}+\boldsymbol{\pi}_1) \\ \overline{\widetilde{m_0}}(\boldsymbol{\omega}+\boldsymbol{\pi}_2) & \overline{\widetilde{m_1}}(\boldsymbol{\omega}+\boldsymbol{\pi}_2) & \dots & \overline{\widetilde{m_6}}(\boldsymbol{\omega}+\boldsymbol{\pi}_2) \\ \vdots & \vdots & \vdots & \vdots \\ 0 & \overline{\widetilde{m_1}}(\boldsymbol{\omega}+\boldsymbol{\pi}_7) & \dots & \overline{\widetilde{m_6}}(\boldsymbol{\omega}+\boldsymbol{\pi}_7) \end{bmatrix} \begin{bmatrix} m_0(\boldsymbol{\omega}) \\ m_1(\boldsymbol{\omega}) \\ m_2(\boldsymbol{\omega}) \\ \vdots \\ m_6(\boldsymbol{\omega}) \end{bmatrix} = \begin{bmatrix} 1 \\ 0 \\ 0 \\ \vdots \\ 0 \end{bmatrix} \tag{18}$$

In summary, the construction of a biorthogonal basis (13) is equivalent to find feasible solutions of (18) with constraint (17).[3] Our approach to this is inspired by the approach in [5] for constructing compactly supported symmetric biorthogonal filters on a hexagon lattice. We next review the main scheme in [5] and adapt it to our setup of biorthogonal bases on the dyadic quincunx lattice.

4.1 Summary of Cohen et al.'s Construction

We summerize the main setup and the approach in [5]. Consider a biorthogonal scheme consisting of three high-pass filters m_1, m_2 and m_3 and a low-pass filter m_0 together with their biorthogonal duals $\widetilde{m_j}$, s.t. m_0 and $\widetilde{m_0}$ are $\frac{2\pi}{3}$-rotation invariant and m_1, m_2, m_3 and their duals are $\frac{2\pi}{3}$-rotation co-variant on a hexagon lattice.

This biorthogonal scheme satisfies the following linear system ([5, Lemma 2.2.2])

$$\begin{bmatrix} \overline{\widetilde{m_0}}(\boldsymbol{\omega}) & \overline{\widetilde{m_1}}(\boldsymbol{\omega}) & \overline{\widetilde{m_2}}(\boldsymbol{\omega}) & \overline{\widetilde{m_3}}(\boldsymbol{\omega}) \\ \overline{\widetilde{m_0}}(\boldsymbol{\omega}+\boldsymbol{\nu}_1) & \overline{\widetilde{m_1}}(\boldsymbol{\omega}+\boldsymbol{\nu}_1) & \overline{\widetilde{m_2}}(\boldsymbol{\omega}+\boldsymbol{\nu}_1) & \overline{\widetilde{m_3}}(\boldsymbol{\omega}+\boldsymbol{\nu}_1) \\ \overline{\widetilde{m_0}}(\boldsymbol{\omega}+\boldsymbol{\nu}_2) & \overline{\widetilde{m_1}}(\boldsymbol{\omega}+\boldsymbol{\nu}_2) & \overline{\widetilde{m_2}}(\boldsymbol{\omega}+\boldsymbol{\nu}_2) & \overline{\widetilde{m_3}}(\boldsymbol{\omega}+\boldsymbol{\nu}_2) \\ \overline{\widetilde{m_0}}(\boldsymbol{\omega}+\boldsymbol{\nu}_3) & \overline{\widetilde{m_1}}(\boldsymbol{\omega}+\boldsymbol{\nu}_3) & \overline{\widetilde{m_2}}(\boldsymbol{\omega}+\boldsymbol{\nu}_3) & \overline{\widetilde{m_3}}(\boldsymbol{\omega}+\boldsymbol{\nu}_3) \end{bmatrix} \begin{bmatrix} m_0(\boldsymbol{\omega}) \\ m_1(\boldsymbol{\omega}) \\ m_2(\boldsymbol{\omega}) \\ m_3(\boldsymbol{\omega}) \end{bmatrix} = \begin{bmatrix} 1 \\ 0 \\ 0 \\ 0 \end{bmatrix}. \tag{19}$$

where $\boldsymbol{\nu}_i = \boldsymbol{\pi}_{2i}$, $i = 1, 2, 3$. Let $\widetilde{\mathbf{M}}(\boldsymbol{\omega}) \in \mathbb{C}^{4\times 4}$ be the matrix with entries $\overline{\widetilde{m_j}}(\boldsymbol{\omega}+\boldsymbol{\nu}_i)$ and $\mathbf{m}(\boldsymbol{\omega}) \in \mathbb{C}^4$ be the vector with entries $m_j(\boldsymbol{\omega})$ in (19), then (19) can be written as

$$\widetilde{\mathbf{M}}(\boldsymbol{\omega})\,\mathbf{m}(\boldsymbol{\omega}) = [1, 0, 0, 0]^\top.$$

Begin with a pre-designed $\widetilde{m_1}(\boldsymbol{\omega})$ with desired propery, $\widetilde{m_2}(\boldsymbol{\omega})$ and $\widetilde{m_3}(\boldsymbol{\omega})$ are determined by symmetry. Lemma 2.2.2 in [5] then leads to

[3] It can be shown that as long as (18) has a unique solution for m_j given fixed $\widetilde{m_j}$, $j = 0, \dots, 6$, (17) always holds. See Sect. 4.2.

$$\begin{aligned} m_0(\boldsymbol{\omega}) &= D^{-1} \begin{vmatrix} \overline{\widetilde{m_1}}(\boldsymbol{\omega}+\boldsymbol{\nu}_1) & \overline{\widetilde{m_2}}(\boldsymbol{\omega}+\boldsymbol{\nu}_1) & \overline{\widetilde{m_3}}(\boldsymbol{\omega}+\boldsymbol{\nu}_1) \\ \overline{\widetilde{m_1}}(\boldsymbol{\omega}+\boldsymbol{\nu}_2) & \overline{\widetilde{m_2}}(\boldsymbol{\omega}+\boldsymbol{\nu}_2) & \overline{\widetilde{m_3}}(\boldsymbol{\omega}+\boldsymbol{\nu}_2) \\ \overline{\widetilde{m_1}}(\boldsymbol{\omega}+\boldsymbol{\nu}_3) & \overline{\widetilde{m_2}}(\boldsymbol{\omega}+\boldsymbol{\nu}_3) & \overline{\widetilde{m_3}}(\boldsymbol{\omega}+\boldsymbol{\nu}_3) \end{vmatrix} \\ &= D^{-1} \widetilde{\mathbf{M}}_{0,0}(\boldsymbol{\omega}), \end{aligned} \tag{20}$$

where $\widetilde{\mathbf{M}}_{0,0}(\boldsymbol{\omega})$ is the minor of $\widetilde{\mathbf{M}}(\boldsymbol{\omega})$ with respect to $\overline{\widetilde{m_0}}(\boldsymbol{\omega})$ and $D \equiv \det(\widetilde{\mathbf{M}}(\boldsymbol{\omega})) \in \mathbb{C}^* = \mathbb{C}\backslash\{0\}$ does not depend on $\boldsymbol{\omega}$ in [5], due to the symmetry of $\widetilde{m_j}$.

Expanding $det(\widetilde{\mathbf{M}}(\boldsymbol{\omega}))$ with respect to the first column leads to the following constraint on $\widetilde{m_0}(\boldsymbol{\omega})$,

$$m_0\overline{\widetilde{m_0}}(\boldsymbol{\omega}) + m_0\overline{\widetilde{m_0}}(\boldsymbol{\omega}+\boldsymbol{\nu}_1) + m_0\overline{\widetilde{m_0}}(\boldsymbol{\omega}+\boldsymbol{\nu}_2) + m_0\overline{\widetilde{m_0}}(\boldsymbol{\omega}+\boldsymbol{\nu}_3) = 1, \tag{21}$$

which is the same as the identity constraint (17) in our setup. Once (21) is solved for $\widetilde{m_0}$, m_1, m_2 and m_3 are obtained by solving the linear system (19) as $\widetilde{\mathbf{M}}(\boldsymbol{\omega})$ has been determined.

4.2 Adaptation to Dyadic Quincunx Downsampling

Cohen et al's approach can be adapted to construct biorthogonal bases in different settings; We shall apply it to our framework, even though we work with different lattices, downsampling schemes and symmetries. In particular, we adapt their approach to solve (18) with constraint (17) where $\widetilde{m_j},\ j = 1, \dots, 6$ are pre-designed. Furthermore, by exploiting the symmetric structure of (18) with respect to the shifts $\boldsymbol{\pi}_i,\ i = 0, \dots, 7$, we derive necessary conditions for (18) to have a unique solution. It turns out that these will, once again, force to exhibit lack of regularity in our biorthogonal scheme.

Since (18) takes the same form as (19), we adopt, for the sake of simplicity and for the rest of this paper, the matrix and vector notations $\widetilde{\mathbf{M}}(\boldsymbol{\omega}),\ \mathbf{m}(\boldsymbol{\omega})$ that helped to simplify (19). Accordingly, we rewrite (18) as

$$\widetilde{\mathbf{M}}(\boldsymbol{\omega})\, \mathbf{m}(\boldsymbol{\omega}) = [1, 0, 0, 0, 0, 0, 0]^\top,$$

where $\widetilde{\mathbf{M}}(\boldsymbol{\omega}) \in \mathbb{C}^{8\times 7}$ and $\mathbf{m}(\boldsymbol{\omega}) \in \mathbb{C}^7$. In addition, let $\boldsymbol{b}_k \in \mathbb{R}^8$, $0 \le k \le 7$, whose only non-zero entry is $\boldsymbol{b}_k[k] = 1$, where the indexing starts with zero. Note that $\widetilde{\mathbf{M}}(\boldsymbol{\omega})\, \mathbf{m}(\boldsymbol{\omega}) = \boldsymbol{b}_0 \in \mathbb{R}^8$ is over-determined; it has a unique solution of m_j if and only if

(5.i) $\widetilde{\mathbf{M}}(\boldsymbol{\omega})$ is full rank,
(5.ii) $[\widetilde{\mathbf{M}}(\boldsymbol{\omega}), \boldsymbol{b}_0]$ is singular,

where we use the notation [ ] for the concatenation of $\widetilde{\mathbf{M}}(\boldsymbol{\omega})$ and $\boldsymbol{b}_0$ into a 8×8 matrix. The matrix $\widetilde{\mathbf{M}}(\boldsymbol{\omega})$ is structured such that each row is associated with a shift $\boldsymbol{\pi}_i,\ i = 0, \dots, 7$ and each column is associated with a dual function $\widetilde{m_j}(\boldsymbol{\omega}),\ j = 0, \dots, 7$. In particular, $\widetilde{\mathbf{M}}(\boldsymbol{\omega})$ depends on the value of $\widetilde{m_j}$ at $\boldsymbol{\omega}$ and its shifts $\boldsymbol{\omega} + \boldsymbol{\pi}_i$. We denote a submatrix of $\widetilde{\mathbf{M}}(\boldsymbol{\omega})$ containing all but the row associated with $\boldsymbol{\pi}_k$ (respectively, the column associated with $\widetilde{m_k}(\boldsymbol{\omega})$) as $\widetilde{\mathbf{M}}[\widehat{k}, :](\boldsymbol{\omega})$ (respectively, $\widetilde{\mathbf{M}}[:, \widehat{k}](\boldsymbol{\omega})$). In particular, we denote $\widetilde{\mathbf{M}}[\widehat{0}, \widehat{0}](\boldsymbol{\omega})$ as $\widetilde{\mathbf{M}}^{\square}(\boldsymbol{\omega})$.

We have the following observations for $\widetilde{\mathbf{M}}(\boldsymbol{\omega})$.

Lemma 4.1 *$\forall \boldsymbol{\omega} \in S_0$, if (18) is solvable, then $\widetilde{\mathbf{M}}[\widehat{0}, :](\boldsymbol{\omega})$ is singular.*

Proof If (18) is solvable, then condition (5.ii) holds, which implies that $\det([\widetilde{\mathbf{M}}(\boldsymbol{\omega}), \boldsymbol{b}_0]) = 0$. Expanding the determinant with respect to the last column $\boldsymbol{b}_0$ yields $\det(\widetilde{\mathbf{M}}[\widehat{0}, :](\boldsymbol{\omega})) = 0$. □

Lemma 4.2 *$\widetilde{\mathbf{M}}(\boldsymbol{\omega})$, $\widetilde{\mathbf{M}}(\boldsymbol{\omega} + \boldsymbol{\pi}_2)$, $\widetilde{\mathbf{M}}(\boldsymbol{\omega} + \boldsymbol{\pi}_4)$ and $\widetilde{\mathbf{M}}(\boldsymbol{\omega} + \boldsymbol{\pi}_6)$ are the same up to row permutations. (18) holds $\forall \boldsymbol{\omega}$ if and only if $\widetilde{\mathbf{M}}(\boldsymbol{\omega})\big[\, \mathbf{m}(\boldsymbol{\omega}), \mathbf{m}(\boldsymbol{\omega} + \boldsymbol{\pi}_2), \mathbf{m}(\boldsymbol{\omega} + \boldsymbol{\pi}_4), \mathbf{m}(\boldsymbol{\omega} + \boldsymbol{\pi}_6) \,\big] = \big[\, \boldsymbol{b}_0, \boldsymbol{b}_2, \boldsymbol{b}_4, \boldsymbol{b}_6 \,\big]$.*

Remark If we consider $\widetilde{\mathbf{M}}(\boldsymbol{\omega})$ a matrix-valued function of $\boldsymbol{\omega}$, then the conditions (5.i) and (5.ii) are both pointwise, yet Lemma 4.2 shows that the set of points $\{\boldsymbol{\omega}, \boldsymbol{\omega} + \boldsymbol{\pi}_2, \boldsymbol{\omega} + \boldsymbol{\pi}_4, \boldsymbol{\omega} + \boldsymbol{\pi}_6\}$ are linked together by the symmetry in $\widetilde{\mathbf{M}}(\boldsymbol{\omega})$.

Due to condition (5.i), for any $\boldsymbol{\omega}$, there exists $k_{\boldsymbol{\omega}}$ depending on $\boldsymbol{\omega}$ such that $\widetilde{\mathbf{M}}[\widehat{k_{\boldsymbol{\omega}}}, :](\boldsymbol{\omega})$ is non-singular. Lemma 4.1 implies that $\widehat{k_{\boldsymbol{\omega}}} \neq 0$[4]; therefore we may apply Cramer's rule to $\widetilde{\mathbf{M}}[\widehat{k_{\boldsymbol{\omega}}}, :](\boldsymbol{\omega})$, as in Sect. 4.1, and obtain the following expression of $m_0(\boldsymbol{\omega})$

$$m_0(\boldsymbol{\omega}) = \det(\widetilde{\mathbf{M}}^{\square}[\widehat{k_{\boldsymbol{\omega}}}, :](\boldsymbol{\omega})) / \det(\widetilde{\mathbf{M}}[\widehat{k_{\boldsymbol{\omega}}}, :](\boldsymbol{\omega})). \tag{22}$$

Moreover, based on (22), the identity condition (17) on $m_0(\boldsymbol{\omega})$ and $\widetilde{m_0}(\boldsymbol{\omega})$ can be derived in the same way as (21) by expanding $\det(\widetilde{\mathbf{M}}[\widehat{k_{\boldsymbol{\omega}}}, :](\boldsymbol{\omega}))$.

4.3 Discontinuity of $\widetilde{m_j}(\boldsymbol{\omega})$

In this subsection, we show our main result that for (18) to be uniquely solvable, the pre-designed $\widetilde{m_j}$ have to be discontinuous as soon as they satisfy mild symmetry conditions and concentration of support on C_j.

We assume that $|\widetilde{m_1}(\boldsymbol{\omega})|$ and $|\widetilde{m_6}(\boldsymbol{\omega})|$ are symmetric with respect to the diagonal $\omega_1 = \omega_2$, i.e.

$$|\widetilde{m_1}(\boldsymbol{\omega})| = |\widetilde{m_6}(\boldsymbol{\omega}')| \quad \forall\, \omega_1 = \omega_2', \quad \omega_2 = \omega_1', \tag{23}$$

and likewise for $\widetilde{m_3}(\boldsymbol{\omega})$ and $\widetilde{m_4}(\boldsymbol{\omega})$,

$$|\widetilde{m_3}(\boldsymbol{\omega})| = |\widetilde{m_4}(\boldsymbol{\omega}')| \quad \forall\, \omega_1 = -\omega_2', \quad \omega_2 = -\omega_1'. \tag{24}$$

In what follows, we introduce a triangular partition of $S_0 = [-\pi, \pi) \times [-\pi, \pi)$ in the frequency plane and define formally the concentration of the support of the $\widetilde{m_j}$.

[4] By symmetry, we have the stronger result $k_{\boldsymbol{\omega}} \notin \{0, 2, 4, 6\}$. Indeed, Lemmas 4.1 and 4.2 together imply that $\widetilde{\mathbf{M}}[\widehat{k}, :](\boldsymbol{\omega})$, $k = 0, 2, 4, 6$ are singular. Therefore, $\widehat{k_{\boldsymbol{\omega}}} \in \{1, 3, 5, 7\}$ and thus $\widetilde{\mathbf{M}}[\widehat{k_{\boldsymbol{\omega}}}, :](\boldsymbol{\omega})$ contains all rows associated with shifts $\boldsymbol{\pi}_{2i}$, $i = 0, \ldots, 3$.

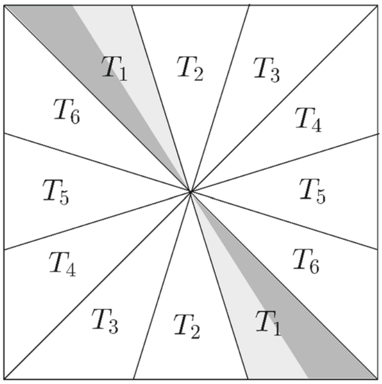

Fig. 3 Partition of frequency square in six directions, where the essential support of $\widetilde{m_i}(\boldsymbol{\omega})$ is contained in each pair of triangles T_i. The *pair of dark grey triangles* is T_1^- and the *light grey pair* is T_1^+

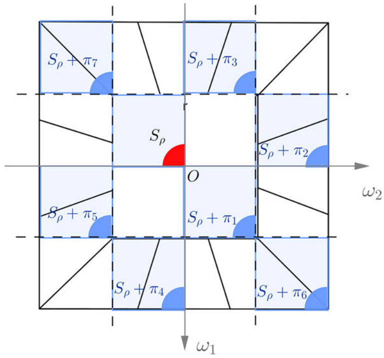

Fig. 4 S_ρ and its shifts

Definition The *domination-support* Ω_j of a function $\widetilde{m_j}$ (with respect to the other $m_i, i \neq j$) is the set $\{\boldsymbol{\omega} : |\widetilde{m_j}(\boldsymbol{\omega})| > |\widetilde{m_i}(\boldsymbol{\omega})|, \forall i \neq j\}$. c.5em

Let T_j be pairs of triangles shown in Fig. 3, defined such that $C_j \subset T_j$, $j = 1, \ldots, 6$. Consider the decompositions $T_j = T_j^- \bigcup T_j^+$, where T_j^-, T_j^+ are halves of T_j adjacent to its neighboring triangles T_i in the counter clockwise and clockwise directions respectively.

Definition $\widetilde{m_j}$ *concentrates* in T_j for $j = 1, \ldots, 6$ if

(i) $\Omega_j \subset T_j$;
(ii) $\mathrm{supp}(\widetilde{m_j}) \subset T_{j-1}^+ \bigcup T_j \bigcup T_{j+1}^-$ and $\int_\Omega |\widetilde{m_j}| > \int_{\Omega'} |\widetilde{m_j}|, \forall\, \Omega \subset T_j \bigcap \mathrm{supp}(\widetilde{m_j})$ s.t. $|\Omega| > 0$, where $\Omega' \subset T_{j-1}^+ \bigcup T_{j+1}^-$ is symmetric to Ω with respect to the boundary of T_j.

In other words, for $\widetilde{m_j}$ to concentrate in T_j, $\widetilde{m_j}$ should be "mainly" supported in T_j (condition (i)) and "decay" properly outside of T_j (condition (ii)).

We say $\widetilde{m_0}$ concentrates in C_0 if $\Omega_0 \subset C_0$. For m_0, we impose the natural requirement that, for some (possibly small) $\rho > 0$, we have $|m_0(\boldsymbol{\omega})| > 0$, $\forall\, |\boldsymbol{\omega}| < \rho$. Given these constraints on the support of $\widetilde{m_j}$ and m_0, we examine the consequences of the singularity condition on $\widehat{\mathbf{M}}[\widehat{0}, :](\boldsymbol{\omega})$ from Lemma 4.1, specifically in the domain $S_\rho = \{(\omega_1, \omega_2) |\, |\boldsymbol{\omega}| < \rho, \omega_1 < 0,\ \omega_2 < 0\}$, see the red zone in Fig. 4.

Let $\widetilde{\mathbf{m}}^i(\boldsymbol{\omega}) = [\widetilde{m_1}(\boldsymbol{\omega}+\boldsymbol{\pi}_i)\ \ldots,\ \widetilde{m_6}(\boldsymbol{\omega}+\boldsymbol{\pi}_i)] \in \mathbb{C}^6$, $i = 0, \ldots, 7$ be the rows of $\widetilde{\mathbf{M}}[:, \widehat{0}](\boldsymbol{\omega})$.

Lemma 4.3 *If* $\boldsymbol{\omega} \in S_\rho$ *s.t.* (17) *holds and* $\widetilde{\mathbf{M}}[\widehat{0}, :](\boldsymbol{\omega})$ *is singular, then* $rank(\widetilde{\mathbf{m}}^1, \widetilde{\mathbf{m}}^7) = 1$ *and* $rank(\widetilde{\mathbf{m}}^3, \widetilde{\mathbf{m}}^5) = 2$ *or* $rank(\widetilde{\mathbf{m}}^3, \widetilde{\mathbf{m}}^5) = 1$ *and* $rank(\widetilde{\mathbf{m}}^1, \widetilde{\mathbf{m}}^7) = 2$.

Lemma 4.3 can be proved by analyzing the linear dependency and independency between the $\widetilde{\mathbf{m}}^i$ on S_ρ, since the $\widetilde{\mathbf{m}}^i$ have known locations of zero entries when ρ is small due to the concentration of the $\widetilde{m_j}$. For the full proof of Lemma 4.3, see Appendix 2.

The concentration of $\widetilde{m_3}(\boldsymbol{\omega})$ and $\widetilde{m_4}(\boldsymbol{\omega})$ in T_3 and T_4 and their symmetry together imply that $rank(\widetilde{\mathbf{m}}^3, \widetilde{\mathbf{m}}^5) \neq 1$ $a.e.$ on S_ρ (see Lemma 9.3 in Appendix "Discontinuity of $\widetilde{m_j}(\boldsymbol{\omega})$" section), hence $rank(\widetilde{\mathbf{m}}^1(\boldsymbol{\omega}), \widetilde{\mathbf{m}}^7(\boldsymbol{\omega})) = 1$ $a.e.$ on S_ρ. Therefore, $\widetilde{m_1}(\boldsymbol{\omega} + \boldsymbol{\pi}_1)$, $\widetilde{m_6}(\boldsymbol{\omega}+\boldsymbol{\pi}_1)$ in $\widetilde{\mathbf{m}}^1(\boldsymbol{\omega})$ and the corresponding $\widetilde{m_1}(\boldsymbol{\omega}+\boldsymbol{\pi}_7)$, $\widetilde{m_6}(\boldsymbol{\omega}+\boldsymbol{\pi}_7)$ in $\widetilde{\mathbf{m}}^7(\boldsymbol{\omega})$ on S_ρ are linearly related. Furthermore, we can show that $\widetilde{m_6}(\boldsymbol{\omega}) = 0$ $a.e.$ on $S_\rho + \boldsymbol{\pi}_1 \cap \{\omega_1 < \omega_2\}$ (see Proposition 9.5 in Appendix "Discontinuity of $\widetilde{m_j}(\boldsymbol{\omega})$" section), if $\widetilde{m_0}(\boldsymbol{\omega})$, $\widetilde{m_1}(\boldsymbol{\omega})$ and $\widetilde{m_6}(\boldsymbol{\omega})$ concentrate in C_0, T_1 and T_6 respectively. Therefore, if $\widetilde{m_6}(\boldsymbol{\omega})$ is continuous, $\widetilde{m_6}(\frac{\pi}{2}, \frac{\pi}{2}) = 0$; the same holds for $\widetilde{m_1}(\boldsymbol{\omega})$ and for $(-\frac{\pi}{2}, -\frac{\pi}{2})$ as well by symmetry. The following theorem summarizes our main result.

Theorem 6 *If the* $\widetilde{m_j}$ *concentrate in* T_j *for* $j = 1, 3, 4, 6$ *with symmetries* (23) *and* (24) *and* $\widetilde{m_0}$ *concentrates in* C_0, *then* $\widetilde{m_1}(\boldsymbol{\omega})$, $\widetilde{m_6}(\boldsymbol{\omega})$ *cannot be continuous at both* $(\frac{\pi}{2}, \frac{\pi}{2})$ *and* $(-\frac{\pi}{2}, -\frac{\pi}{2})$ *for* (18) *to have a unique solution of* m_j *such that there exists* $\rho > 0$, $m_0(\boldsymbol{\omega})$ *is non-zero on* $|\boldsymbol{\omega}| < \rho$.

Proof If $\widetilde{m_1}(\boldsymbol{\omega})$ and $\widetilde{m_6}(\boldsymbol{\omega})$ are both continuous at $(\frac{\pi}{2}, \frac{\pi}{2})$ and $(-\frac{\pi}{2}, -\frac{\pi}{2})$, then $\widetilde{m_1}(\frac{\pi}{2}, \frac{\pi}{2}) = \widetilde{m_1}(-\frac{\pi}{2}, -\frac{\pi}{2}) = \widetilde{m_6}(\frac{\pi}{2}, \frac{\pi}{2}) = \widetilde{m_6}(-\frac{\pi}{2}, -\frac{\pi}{2}) = 0$. Therefore, $\widetilde{\mathbf{m}}^1(\mathbf{0}) = \widetilde{\mathbf{m}}^7(\mathbf{0}) = \mathbf{0}$ at the origin which results in contradiction with Lemma 4.3. □

5 Numerical Construction of Biorthogonal Bases

In this section, we develop a numerical construction of biorthogonal bases on a dyadic quincunx lattice following an approach similar to Cohen et al. We first design $\widetilde{m_j}(\boldsymbol{\omega})$, $j = 1, \ldots, 6$, on the canonical frequency square $S_0 = [-\pi, \pi) \times [-\pi, \pi)$ associated with the lattice $\mathbb{Z}^2$, then solve for m_0, $\widetilde{m_0}$ and m_j on S_0 in order with respect to (18) and (17).

5.1 Design of Input $\widetilde{m_j}(\omega)$

In this sub-section, we construct $\widetilde{m_j}(\boldsymbol{\omega})$, $j = 1, \ldots, 6$, which concentrate in T_i. Specifically, following the orthonormal construction in [16], we consider $\widetilde{m_j}(\boldsymbol{\omega})$ in the form

$$\widetilde{m_j}(\boldsymbol{\omega}) = e^{-i\boldsymbol{\eta}_j^\top \boldsymbol{\omega}} |\widetilde{m_j}(\boldsymbol{\omega})|, \quad j = 1, \ldots, 6, \tag{25}$$

where $\boldsymbol{\eta}_j \in \mathbb{Z}^2$ is the phase constant of $\widetilde{m_j}$. In addition to the symmetry of pairs $(|\widetilde{m_1}|, |\widetilde{m_6}|)$ and $(|\widetilde{m_3}|, |\widetilde{m_4}|)$ assumed in Sect. 4.3, we further require that $|\widetilde{m_2}|$ and $|\widetilde{m_5}|$ are symmetric with respect to the ω_1-axis and ω_2-axis accordingly. Figure 5 shows a design of $|\widetilde{m_j}(\boldsymbol{\omega})|$ that has these strong symmetries.

The symmetries of $(|\widetilde{m_1}|, |\widetilde{m_6}|)$ leads to constraints on the phase constants $\boldsymbol{\eta}_j$ introduced in (25).

Lemma 5.1 *If there exists* $\boldsymbol{\omega} \in D_1 := \{\omega_1 = \omega_2,\ \omega_1 \in (-\frac{\pi}{2}, 0)\}$, *s.t.* $|m_0(\boldsymbol{\omega})| \neq 0$, *then* $(\boldsymbol{\eta}_1 - \boldsymbol{\eta}_6)^\top(\boldsymbol{\pi}_6 - \boldsymbol{\pi}_7) \neq 0(mod\, 2\pi)$.

Because $m_0(\boldsymbol{\omega})$ can be expressed as in (22), $|m_0(\boldsymbol{\omega})| \neq 0$ is equivalent to $\det(\widetilde{\mathbf{M}}^\square[\widehat{k_{\boldsymbol{\omega}}}, :](\boldsymbol{\omega})) \neq 0$, i.e. $\widetilde{\mathbf{M}}^\square(\boldsymbol{\omega})$ is full rank. The constraint on $\boldsymbol{\eta}_1$ and $\boldsymbol{\eta}_6$ then follows from substituting non-zero entries of $\widetilde{\mathbf{M}}^\square(\boldsymbol{\omega})$ by (25) and consider the linear dependency of the columns in $\widetilde{\mathbf{M}}^\square(\boldsymbol{\omega})$. For the full proof of Lemma 5.1, see Appendix "Design of Input $\widetilde{m_j}(\boldsymbol{\omega})$" section.

Similarly, if there exists $\boldsymbol{\omega} \in \{\omega_1 = \omega_2,\ \omega_1 \in (0, \frac{\pi}{2})\}$, *s.t.* $|m_0(\boldsymbol{\omega})| \neq 0$, then $(\boldsymbol{\eta}_1 - \boldsymbol{\eta}_6)^\top(\boldsymbol{\pi}_6 - \boldsymbol{\pi}_1) \neq 0(\mathrm{mod}\, 2\pi)$. These two conditions are equivalent to

$$(\boldsymbol{\eta}_1 - \boldsymbol{\eta}_6)^\top(\pi/2, \pi/2) \neq 0(\mathrm{mod}\, 2\pi) \tag{c1.1}$$

since $\boldsymbol{\eta}_1,\ \boldsymbol{\eta}_6 \in \mathbb{Z}^2$. Considering the other diagonal segment $\{\omega_2 = -\omega_1, |\omega_1| < \frac{\pi}{2}\}$ and the symmetry of $(|\widetilde{m_3}|, |\widetilde{m_4}|)$, we similarly obtain

$$(\boldsymbol{\eta}_3 - \boldsymbol{\eta}_4)^\top(-\pi/2, \pi/2) \neq 0(\mathrm{mod}\, 2\pi) \tag{c1.2}$$

Next, we consider $\widetilde{m_0}(\mathbf{0})$ and investigate $\widetilde{\mathbf{M}}^\square(\boldsymbol{\omega})$ at the origin.

Proposition 5.2 *If* $|\widetilde{m_0}(\mathbf{0})| \neq 0$, *then* $\boldsymbol{\pi}_1^\top(\boldsymbol{\eta}_1 - \boldsymbol{\eta}_6) \neq \pi(mod\, 2\pi)$ *or* $\boldsymbol{\pi}_3^\top(\boldsymbol{\eta}_3 - \boldsymbol{\eta}_4) \neq \pi(mod\, 2\pi)$.

Remark The proof of Proposition 5.2 is similar to that of Lemma 5.1 but more involved. See Appendix "Design of Input $\widetilde{m_j}(\boldsymbol{\omega})$" section for the full proof.

We propose the following set of phases such that (c1.1) and (c1.2) as well as the necessary condition from Proposition 5.2 are all satisfied,

$$\begin{aligned} &\boldsymbol{\eta}_1 = (0, 0),\ \ \boldsymbol{\eta}_2 = (-1, 1),\ \ \boldsymbol{\eta}_3 = (0, 2), \\ &\boldsymbol{\eta}_4 = (1, 0),\ \ \boldsymbol{\eta}_5 = (0, -1),\ \ \boldsymbol{\eta}_6 = (0, 1). \end{aligned} \tag{26}$$

The design of $\widetilde{m_j}(\boldsymbol{\omega})$ in the form of (25) with phases (26) introduced here do not guarantee that (18) has a unique solution. We will see the necessary and sufficient conditions that $\widetilde{m_j}(\boldsymbol{\omega})$ have to satisfy in the next subsection given by Proposition 5.3.

5.2 Solving (18) and (17) for m_0, $\widetilde{m_0}$ and m_j

Once $\widetilde{m_j}(\boldsymbol{\omega})$, $j = 1, \ldots, 6$ are fixed on S_0, (18) can be reformulated as follows,

$$\widetilde{\mathbf{M}}[:, \widehat{0}](\boldsymbol{\omega}) \begin{bmatrix} m_1(\boldsymbol{\omega}) \\ m_2(\boldsymbol{\omega}) \\ m_3(\boldsymbol{\omega}) \\ m_4(\boldsymbol{\omega}) \\ m_5(\boldsymbol{\omega}) \\ m_6(\boldsymbol{\omega}) \end{bmatrix} = \boldsymbol{b}_0 - m_0(\boldsymbol{\omega}) \begin{bmatrix} \overline{\widetilde{m_0}}(\boldsymbol{\omega}) \\ 0 \\ \overline{\widetilde{m_0}}(\boldsymbol{\omega}+\boldsymbol{\pi}_2) \\ 0 \\ \overline{\widetilde{m_0}}(\boldsymbol{\omega}+\boldsymbol{\pi}_4) \\ 0 \\ \overline{\widetilde{m_0}}(\boldsymbol{\omega}+\boldsymbol{\pi}_6) \\ 0 \end{bmatrix} \doteq \boldsymbol{b}_0'(\boldsymbol{\omega}), \tag{27}$$

where $\widetilde{\mathbf{M}}[:, \widehat{0}](\boldsymbol{\omega})$ is completely determined by $\widetilde{m_j}(\boldsymbol{\omega})$, $j = 1, \ldots, 6$ and m_j, $j = 1, \ldots, 6$ can be uniquely solved on S_0 if and only if $\forall \boldsymbol{\omega} \in S_0$

(5.2.i) $\widetilde{\mathbf{M}}[:, \widehat{0}](\boldsymbol{\omega})$ is full rank,
(5.2.ii) $\boldsymbol{b}_0'(\boldsymbol{\omega})$ is in $col\big(\widetilde{\mathbf{M}}[:, \widehat{0}](\boldsymbol{\omega})\big)$, the column space of $\widetilde{\mathbf{M}}[:, \widehat{0}](\boldsymbol{\omega})$.

Next, we show that (5.2.ii) breaks down to constraints on two submatrices of $\widetilde{\mathbf{M}}[:, \widehat{0}](\boldsymbol{\omega})$ and quadruples $\big(m_0(\boldsymbol{\omega}), m_0(\boldsymbol{\omega}+\boldsymbol{\pi}_2), m_0(\boldsymbol{\omega}+\boldsymbol{\pi}_4), m_0(\boldsymbol{\omega}+\boldsymbol{\pi}_6)\big)$, $\big(m_0(\boldsymbol{\omega}+\boldsymbol{\pi}_1), m_0(\boldsymbol{\omega}+\boldsymbol{\pi}_3), m_0(\boldsymbol{\omega}+\boldsymbol{\pi}_5), m_0(\boldsymbol{\omega}+\boldsymbol{\pi}_7)\big)$.

Proposition 5.3 *Let $\widetilde{\mathbf{M}}[odd, \widehat{0}](\boldsymbol{\omega}), \widetilde{\mathbf{M}}[even, \widehat{0}](\boldsymbol{\omega}) \in \mathbb{C}^{4\times 6}$ be the submatrices of $\widetilde{\mathbf{M}}[:, \widehat{0}](\boldsymbol{\omega})$ consisting of odd and even indexed rows respectively. For any $\boldsymbol{\omega} \in S_0$, suppose (5.2.i) holds, then (5.2.ii) holds if and only if $rank(\widetilde{\mathbf{M}}[odd, \widehat{0}](\boldsymbol{\omega})) = rank(\widetilde{\mathbf{M}}[even, \widehat{0}](\boldsymbol{\omega})) = 3$ and*

$$[m_0(\boldsymbol{\omega}), m_0(\boldsymbol{\omega}+\boldsymbol{\pi}_2), m_0(\boldsymbol{\omega}+\boldsymbol{\pi}_4), m_0(\boldsymbol{\omega}+\boldsymbol{\pi}_6)]\, \widetilde{\mathbf{M}}[even, \widehat{0}](\boldsymbol{\omega}) = \mathbf{0}, \tag{28}$$

$$[m_0(\boldsymbol{\omega}+\boldsymbol{\pi}_1), m_0(\boldsymbol{\omega}+\boldsymbol{\pi}_3), m_0(\boldsymbol{\omega}+\boldsymbol{\pi}_5), m_0(\boldsymbol{\omega}+\boldsymbol{\pi}_7)]\, \widetilde{\mathbf{M}}[odd, \widehat{0}](\boldsymbol{\omega}) = \mathbf{0}. \tag{29}$$

For the proof of Proposition 5.3, see Appendix "Solving (18) and (17) for m_0, $\widetilde{m_0}$ and m_j" section.

Remark Note that the submatrices $\widetilde{\mathbf{M}}[odd, \widehat{0}](\boldsymbol{\omega})$ and $\widetilde{\mathbf{M}}[even, \widehat{0}](\boldsymbol{\omega})$ are dual to each other under the shift of variable $\boldsymbol{\omega} \mapsto \boldsymbol{\omega}+\boldsymbol{\pi}_i$, when i is odd. Therefore, the constraints $rank(\widetilde{\mathbf{M}}[even, \widehat{0}](\boldsymbol{\omega})) = 3$ and (28) from Proposition 5.3 are sufficient for (5.2.ii) to hold on S_0. Furthermore, because $\widetilde{\mathbf{M}}[even, \widehat{0}](\boldsymbol{\omega})$ and $(\boldsymbol{\omega}, \boldsymbol{\omega}+\boldsymbol{\pi}_2, \boldsymbol{\omega}+\boldsymbol{\pi}_4, \boldsymbol{\omega}+\boldsymbol{\pi}_6)$ are invariant to the shift of variable $\boldsymbol{\omega} \mapsto \boldsymbol{\omega}+\boldsymbol{\pi}_i$ when i is even, we only need to consider the constraints above on the subset $[-\pi, 0) \times [-\pi, 0)$ of S_0.

In summary, $\widetilde{\mathbf{M}}[:, \widehat{0}](\boldsymbol{\omega})$ (or equivalently $\widetilde{m_j}$) has to satisfy the following rank constraints on $[-\pi, 0) \times [-\pi, 0)$ for (27) to be uniquely solvable on S_0,

$$rank\left(\widetilde{\mathbf{M}}[:, \widehat{0}](\boldsymbol{\omega})\right) = 6,\ rank\left(\widetilde{\mathbf{M}}[even, \widehat{0}](\boldsymbol{\omega})\right) = 3. \tag{30}$$

In practice, the rank constraints are hard to impose while designing $\widetilde{m}_j$, in our numerical experiments, we therefore first construct $\widetilde{m}_j$ following the design in Sect. 5.1 and then check if these rank constraints are satisfied, see step 1. in Algorithm 1.

If (30) holds, the vector $[\, m_0(\boldsymbol{\omega}), m_0(\boldsymbol{\omega}+\boldsymbol{\pi}_2), m_0(\boldsymbol{\omega}+\boldsymbol{\pi}_4), m_0(\boldsymbol{\omega}+\boldsymbol{\pi}_6)\,]$ can be uniquely determined by (28) *up to a constant factor* $a_{\boldsymbol{\omega}}$, since it is orthogonal to the column space of $\widetilde{\mathbf{M}}[even, \widehat{0}](\boldsymbol{\omega})$ of co-dimension 1. In particular, we obtain $m_0(\boldsymbol{\omega})$ on S_0 by solving (28) independently at each $\boldsymbol{\omega}$ on $[-\pi, 0) \times [-\pi, 0)$, see step 2. in Algorithm 1. As the constant $a_{\boldsymbol{\omega}}$ can change drastically as $\boldsymbol{\omega}$ changes, there is potential lack of regularity of $m_0(\boldsymbol{\omega})$ as an artifact of the algorithm. Figure 6 shows an $m_0(\boldsymbol{\omega})$ computed in this way, which has discontinuous phase due to $a_{\boldsymbol{\omega}}$. Fortunately, this irregularity is an artifact that can be removed as suggested by the following proposition.

Proposition 5.4 *If* $\widetilde{m}_j(\boldsymbol{\omega}), m_j(\boldsymbol{\omega}),\ j = 0, 1, \ldots, 6$ *satisfy* (18) *and* (17)*, then* $m_0'(\boldsymbol{\omega}) \doteq m_0(\boldsymbol{\omega})c(\boldsymbol{\omega}), \widetilde{m}_0{}'(\boldsymbol{\omega}) \doteq \widetilde{m}_0(\boldsymbol{\omega})\overline{c}(\boldsymbol{\omega})^{-1}$ *together with the same* $m_j(\boldsymbol{\omega}), \widetilde{m}_j(\boldsymbol{\omega})$, $j = 1, \ldots, 6$ *satisfy* (18) *and* (17) *if* $c(\boldsymbol{\omega}) = c(\boldsymbol{\omega}+\boldsymbol{\pi}_2) = c(\boldsymbol{\omega}+\boldsymbol{\pi}_4) = c(\boldsymbol{\omega}+\boldsymbol{\pi}_6) \neq 0$*, i.e.* $c(\boldsymbol{\omega})$ *is* π*-periodic in both* ω_1 *and* ω_2*.*

Proof It follows from the observation that $m_0'(\boldsymbol{\omega})\overline{\widetilde{m}_0{}'}(\boldsymbol{\omega}+\boldsymbol{\pi}_i) = m_0(\boldsymbol{\omega})\overline{\widetilde{m}_0}(\boldsymbol{\omega}+\boldsymbol{\pi}_i)$, when i is even. □

Remark In practice, we use Proposition 5.4 compensate for irregularities introduced by the arbitrary $a_{\boldsymbol{\omega}}$; After $m_0(\boldsymbol{\omega})$ is solved, we can choose $c(\boldsymbol{\omega})$ π-periodic in both ω_1, ω_2 such that $m_0'(\boldsymbol{\omega})$ has improved regularity and use $m_0'(\boldsymbol{\omega})$ as the "regularized" $m_0(\boldsymbol{\omega})$ for the rest of the construction.

To obtain $\widetilde{m}_0(\boldsymbol{\omega})$ on S_0, we solve the identity condition (17) on $[-\pi, 0) \times [-\pi, 0)$ for the quadruple $(\widetilde{m}_0(\boldsymbol{\omega}), \widetilde{m}_0(\boldsymbol{\omega}+\boldsymbol{\pi}_2), \widetilde{m}_0(\boldsymbol{\omega}+\boldsymbol{\pi}_4), \widetilde{m}_0(\boldsymbol{\omega}+\boldsymbol{\pi}_6))$. Note that (17) is the same as (21) in Sect. 4.1. According to Lemma 3.2.1 in [5], by *Hilbert's Nullstellensatz* (21) has a solution if and only if there does not exist $(z_1, z_2) \in (\mathbb{C}^*)^2$, $\mathbb{C}^* = \mathbb{C}\backslash\{0\}$ s.t. $(\pm z_1, \pm z_2)$ are all vanishing points of the z-transform of m_0. Unfortunately this is not very constructive: in general, there is no efficient algorithm to solve *Hilbert's Nullstellensatz*.

Our approach here is to reformulate solving $\widetilde{m}_0(\boldsymbol{\omega})$ under the condition (17) as an optimization problem where (17) serves as a linear constraint. In particular, on a $2N \times 2N$ regular grid $\mathcal{G} = \{\boldsymbol{\omega}_i\}_{i=1}^{4N^2}$ of $[-\pi, \pi) \times [-\pi, \pi)$, (17) can be rewritten as

$$\boldsymbol{A}\,\overline{\widetilde{\mathbf{m}}_0} = \mathbf{1}_{N^2}, \tag{31}$$

where $\widetilde{\mathbf{m}}_0 = [\widetilde{m}_0(\boldsymbol{\omega}_i)]_{i=1}^{4N^2}$ and $\boldsymbol{A} \in \mathbb{C}^{N^2 \times 4N^2}$ is a sparse matrix with entries

$$\boldsymbol{A}_{i,j} = m_0(\boldsymbol{\omega}_j) \sum_{k=0}^{3} \delta(\boldsymbol{\omega}_j - \boldsymbol{\omega}_i - \boldsymbol{\pi}_{2k}), \quad \boldsymbol{\omega}_j \in [-\pi, 0) \times [-\pi, 0).$$

Note that $m_0(\boldsymbol{\omega})$ in $\boldsymbol{A}$ here has been regularized by $c(\boldsymbol{\omega})$, hence we expect the corresponding $\widetilde{m}_0(\boldsymbol{\omega})$ that satisfies (17) (or equivalently (31) on the grid $\mathcal{G}$) to be regular as well. To optimize the regularity of $\widetilde{m}_0(\boldsymbol{\omega})$, we choose the squared ℓ_2 norm of the gradient of $\widetilde{m_0}(\boldsymbol{\omega})$ as the objective function, although other forms of regularity may be imposed by different objective functions.

We thus solve the following quadratic minimization problem with linear constraint,

$$\min_{\mathbf{x}} \ \|\boldsymbol{D}\mathbf{x}\|^2, \quad s.t. \ \boldsymbol{A}\mathbf{x} = \mathbf{1}, \tag{32}$$

where $\boldsymbol{D}$ is the gradient operator, $\circ$ is the Hadamard product and $\boldsymbol{A}$ is the linear operator from (17).

Supplementary numerical results on solving $\widetilde{m_0}(\boldsymbol{\omega})$ by optimization are provided in Appendix 4, where we test this optimization method on known biorthogonal filters m_0 and $\widetilde{m_0}$ and compare the solution from the optimization with the ground truth.

Finally, we plug $m_0(\boldsymbol{\omega})$ and $\widetilde{m_0}(\boldsymbol{\omega})$ into $\boldsymbol{b}_0'(\boldsymbol{\omega})$ on the right of (27) and solve the linear system for the m_j, which has a guaranteed unique solution.

To sum up, we propose Algorithm 1 for biorthogonal directional filter construction with dyadic quincunx downsampling scheme.

Algorithm 1 Construction of m_0, $\widetilde{m_0}$ and $\widetilde{m_j}$ in biorthogonal basis

Input: $\widetilde{m_j}(\boldsymbol{\omega}),\ j = 1, \ldots, 6$, a $2N \times 2N$ regular grid $\mathcal{G} = \{\boldsymbol{\omega}_i\}_{i=1}^{4N^2}$ over $[-\pi, \pi) \times [-\pi, \pi)$,
step 1. construct $\widetilde{\mathbf{M}}[:, \widehat{0}](\boldsymbol{\omega})$ on the subgrid $[-\pi, 0) \times [-\pi, 0)$ and check rank constraints (30),
step 2. solve quadruple $\big(m_0(\boldsymbol{\omega}), m_0(\boldsymbol{\omega} + \boldsymbol{\pi}_2), m_0(\boldsymbol{\omega} + \boldsymbol{\pi}_4), m_0(\boldsymbol{\omega} + \boldsymbol{\pi}_6)\big)$ using (28) on the subgrid in $[-\pi, 0) \times [-\pi, 0)$,
step 3. choose appropriate π-periodic $c(\boldsymbol{\omega})$ and replace $m_0(\boldsymbol{\omega})$ by $m_0'(\boldsymbol{\omega}) = c(\boldsymbol{\omega})m_0(\boldsymbol{\omega})$,
step 4. solve the optimization (32) for $\widetilde{m_0}(\boldsymbol{\omega})$ on $[-\pi, \pi) \times [-\pi, \pi)$,
step 5. solve the reduced linear system (27) for $m_j(\boldsymbol{\omega}),\ j = 1, \ldots, 6$.

Remarks 1. Since $\widetilde{m_j},\ j = 1, \ldots, 6$ are pre-designed, it is relatively easy to control their regularity. In addition, the regularity of $\widetilde{m_0}$ is optimized by (32). Therefore, according to (14), we may hope to obtain dual wavelets with good regularity.

2. In principle, one could formulate an optimization for $c(\boldsymbol{\omega})$ in step 3. and $\widetilde{m_0}(\boldsymbol{\omega})$ in step 4. jointly in order to obtain optimal smoothness for $\widetilde{m_0}(\boldsymbol{\omega})$ given $m_0(\boldsymbol{\omega})$ solved in step 2. Instead of solving a linearly constrained quadratic program like (32), one solves a *quadratically* constrained quadratic program (QCQP), which is non-convex and in general NP-hard. Such a QCQP can be relaxed to a convex semidefinite program (SDP) that can be efficiently solved although the solution is not exact. See Appendix 3 for more details. In Sect. 6, we discuss how to choose $c(\boldsymbol{\omega})$ for an $m_0(\boldsymbol{\omega})$ solved from a specific set of input $\widetilde{m_j}$.
3. Once can also manipulate pairs of $(m_j, \widetilde{m_j})$ according to the generalization of Proposition 5.4 below.

Proposition 5.5 *If* $\widetilde{m_j}(\boldsymbol{\omega}), m_j(\boldsymbol{\omega}),\ j = 0, 1, \ldots, 6$ *satisfy* (18) *and* (17), $m_j^c(\boldsymbol{\omega}) \doteq m_j(\boldsymbol{\omega})c_j(\boldsymbol{\omega}), \widetilde{m_j}^c(\boldsymbol{\omega}) \doteq \widetilde{m_j}(\boldsymbol{\omega})\overline{c_j}(\boldsymbol{\omega})^{-1}$ $j = 0, \ldots, 6$ *satisfy* (18) *and* (17) *if* $c_0(\boldsymbol{\omega}) =$

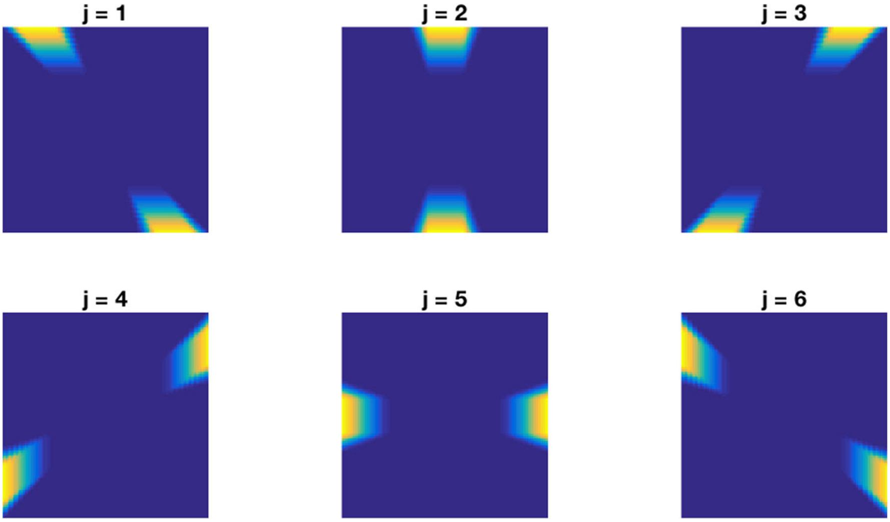

Fig. 5 *First row* input $|\widetilde{m_j}|$ in the vertical cone constructed by shearing the vertical generator (*middle*). *Second row* input $|\widetilde{m_j}|$ in the horizontal cone constructed by rotation of those in the vertical cone

$c_0(\boldsymbol{\omega} + \boldsymbol{\pi}_{2k})$, *for* $k = 0, \ldots, 3$ *and* $c_j(\boldsymbol{\omega}) = c_j(\boldsymbol{\omega} + \boldsymbol{\pi}_k)$, *for* $k = 0, \ldots, 7$, $j = 1, \ldots, 6$.

6 Numerical Experiments

In this section, we demonstrate the numerical construction of biorthogonal directional wavelets on a quincunx lattice using our proposed Algorithm 1 implemented in Matlab.

For the input of Algorithm 1, we use $\widetilde{m_j}$ in the form of (25), with phases in (26) and amplitudes $|\widetilde{m_j}|$ shown in Fig. 5 constructed as follows. We start with a symmetric $|\widetilde{m_2}|$, then compute $|\widetilde{m_1}|$ and $|\widetilde{m_3}|$ by shearing $|\widetilde{m_2}|$ counter-clockwise and clockwise respectively. $|\widetilde{m_4}|$, $|\widetilde{m_5}|$ and $|\widetilde{m_6}|$ are obtained by symmetry with respect to the diagonal. This is the same approach used in the shearlet construction in [12]. Furthermore, we set $\widetilde{m_j}(\boldsymbol{\omega}) = 0$, for all $\boldsymbol{\omega} \in C_0 = [-\pi/2, \pi/2) \times [-\pi/2, \pi/2)$ and according to Theorem 6, we enforce $|\widetilde{m_1}(\frac{\pi}{2}, \frac{\pi}{2})| \neq 0$ and $|\widetilde{m_6}(\frac{\pi}{2}, \frac{\pi}{2})| \neq 0$. As the first step, we numerically verify that this particular design of $\widetilde{m_j}$ satisfies the rank constraints (30).[5]

We proceed to solve $m_0(\boldsymbol{\omega})$ in quadruple separately for each $\boldsymbol{\omega}$ in $[-\pi, 0) \times [-\pi, 0)$. As pointed out earlier, these solutions still have an unconstrained degree of freedom in the form of a constant $a_{\boldsymbol{\omega}}$; the result is shown in Fig. 6 for one implementation using Matlab solvers. This solution $m_0(\boldsymbol{\omega})$ has both inherent irregularity of the biorthogonal construction from the input and artificial irregularity from the algorithm: the amplitude $|m_0(\boldsymbol{\omega})|$ is supported on C_0, where $|m_0(\boldsymbol{\omega})| = 1$ and its discontinuity at ∂C_0

[5] In practice, we find it hard for $\widetilde{m_j}$ to satisfy the rank constraint (30) without enforcing $\widetilde{m_j}$ to be zero on C_0. This may indicate topological obstruction in our biorthogonal scheme.

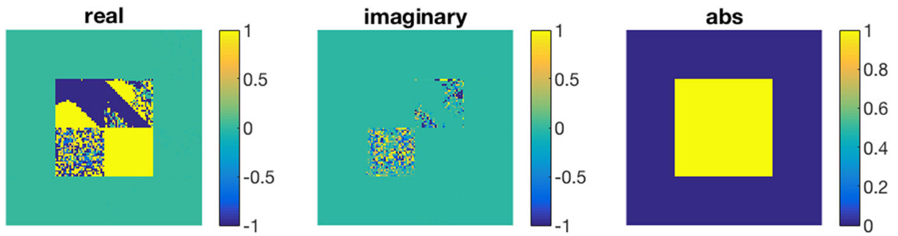

Fig. 6 $m_0(\boldsymbol{\omega})$ constructed from $\widetilde{m}_j$. *Left to right* $Re(m_0(\boldsymbol{\omega}))$, $Im(m_0(\boldsymbol{\omega}))$ and $|m_0(\boldsymbol{\omega})|$

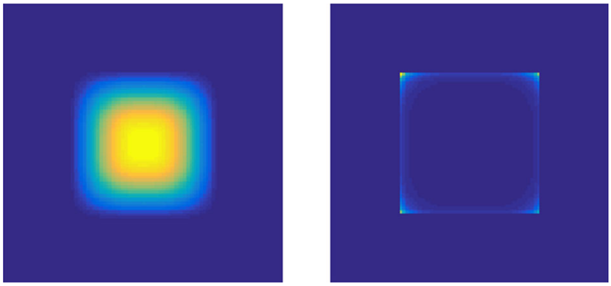

Fig. 7 *Left* $\widetilde{m_0}$, designed smooth function supported on the central square C_0, *right* m_0', where $\overline{m_0'}\widetilde{m_0}(\boldsymbol{\omega}) = \mathbb{1}_{C_0}(\boldsymbol{\omega})$

corresponds to that of the input $\widetilde{m}_j(\boldsymbol{\omega})$; however, the phase of $m_0(\boldsymbol{\omega})$ is discontinuous even on the interior of C_0 due to $a_{\boldsymbol{\omega}}$, an artificial irregularity we remove in the next step by introducing $c(\boldsymbol{\omega})$.

To regularize $m_0(\boldsymbol{\omega})$, we multiply it by an appropriate π-periodic $c(\boldsymbol{\omega})$. In particular, we can first construct $c(\boldsymbol{\omega})$ on C_0 freely and then extend it to S_0 by its π-periodicity in both ω_1 and ω_2. It turns out that in this specific numerical example we consider here, we can explicitly design the regularized $m_0(\boldsymbol{\omega})$ ($m_0'(\boldsymbol{\omega})$) and the corresponding $\widetilde{m_0}(\boldsymbol{\omega})$. Since m_0 is only supported on C_0, $m_0'(\boldsymbol{\omega}) = m_0(\boldsymbol{\omega})c(\boldsymbol{\omega})$ is determined by the value of $c(\boldsymbol{\omega})$ on C_0. Therefore, $m_0'(\boldsymbol{\omega})$ can be any continuous function on C_0. On the other hand, $m_0'\overline{\widetilde{m_0}}(\boldsymbol{\omega}) \equiv 0$, for all $\boldsymbol{\omega} \notin C_0$, and (17) (correspondingly the linear constraint (31)) reduces to $m_0'\overline{\widetilde{m_0}}(\boldsymbol{\omega}) = 1$, for all $\boldsymbol{\omega} \in C_0$. In other words, $\widetilde{m_0}(\boldsymbol{\omega})$ is uniquely determined on C_0 by $m_0'(\boldsymbol{\omega})$ or vice versa. Because we want $\widetilde{m_0}(\boldsymbol{\omega})$ to be smooth and has fast decay from the origin such that the corresponding dual wavelets $\widetilde{\psi}^j$ have good spatial locality, we can actually first design $\widetilde{m_0}(\boldsymbol{\omega})$ on S_0 and then construct $m_0'(\boldsymbol{\omega}) = \widetilde{m_0}(\boldsymbol{\omega})^{-1}$ on C_0. In particular, we let $\widetilde{m_0}$ be the low pass filter of a 2D tensor wavelets, see Fig. 7.

Remarks 1. If we use the above m_0' derived from a known $\widetilde{m_0}(\boldsymbol{\omega})$ and solve (32) for $\widetilde{m_0}(\boldsymbol{\omega})$ as in step 4. of Algorithm 1, we obtain a solution $\widetilde{m_0}'(\boldsymbol{\omega})$ not exactly the same but close to the known $\widetilde{m_0}(\boldsymbol{\omega})$. Moreover, we numerically verify that $m_0'(\boldsymbol{\omega})\overline{\widetilde{m_0}'}(\boldsymbol{\omega}) = \mathbb{1}_{C_0}$ as they should be.

2. There is no restriction on the support of $\widetilde{m_0}(\boldsymbol{\omega})$ as long as (17) is satisfied. Although a slower decay of $\widetilde{m_0}(\boldsymbol{\omega})$ on S_0 increases the regularity $m_0'(\boldsymbol{\omega})$ on C_0, see Fig. 8,

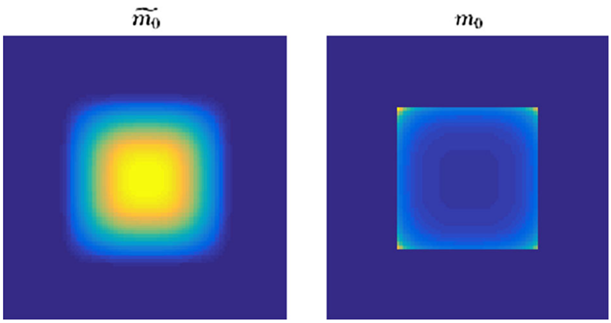

Fig. 8 *Left* $\widetilde{m_0}$, with support outside C_0, *right* m_0', where $\overline{m_0'}\widetilde{m_0}(\boldsymbol{\omega}) = \mathbb{1}_{C_0}(\boldsymbol{\omega})$

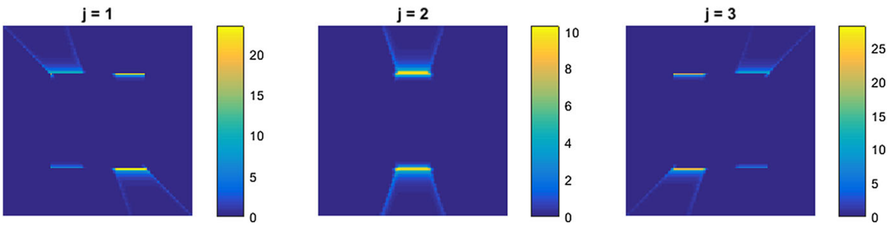

Fig. 9 $|m_j(\boldsymbol{\omega})|$ solved from (27) given $\widetilde{m_j}$ in Fig. 5, m_0' and $\widetilde{m_0}$ in Fig. 8

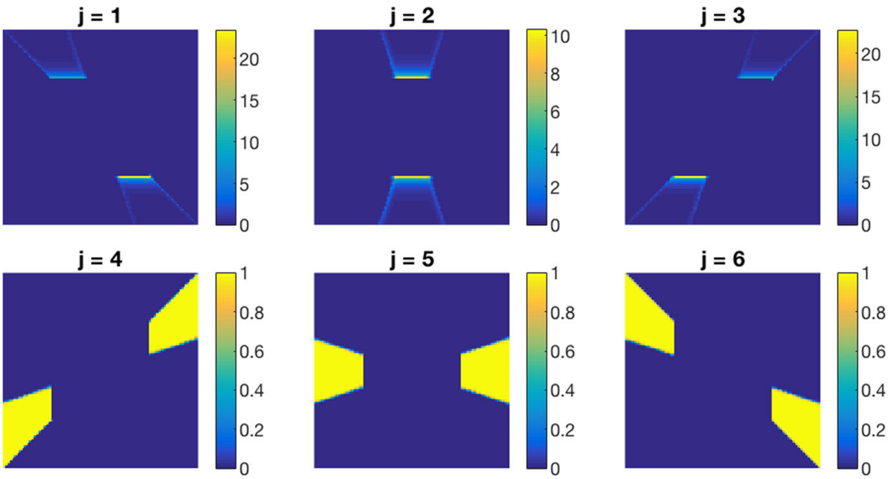

Fig. 10 *Top* $|m_j(\boldsymbol{\omega})|$, $j = 1, 2, 3$, *Bottom* $|m_j(\boldsymbol{\omega})\widetilde{m_j}(\boldsymbol{\omega})|$, $j = 4, 5, 6$, where $m_j(\boldsymbol{\omega})$ is solved from (27) given $\widetilde{m_j}$ in Fig. 5, m_0' and $\widetilde{m_0}$ in Fig. 7

the resulting m_j solved in the final step do not have ideal direction selectivity, see Fig. 9.

Finally, we solve (27) for m_j. As shown in the top row Fig. 10, the energy of m_j concentrates at ∂C_0, where m_j decay to near zero. Moreover, the bottom row of Fig. 10 shows that $|m_j\widetilde{m_j}(\boldsymbol{\omega})|$ are close to constant on C_j. Such irregularity roots in the

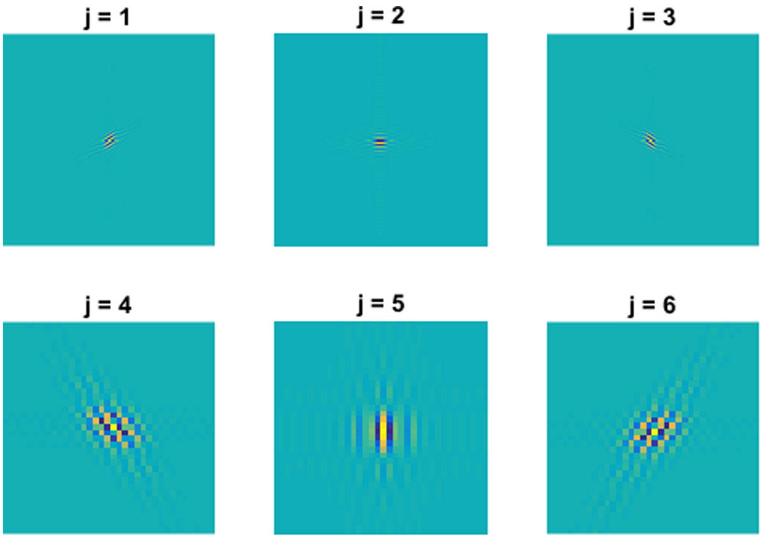

Fig. 11 Real part of $\widetilde{\psi}^j$ constructed from $\widetilde{m_j}$, $j = 1, \ldots, 6$ in Fig. 5 and $\widetilde{m_0}'$ in Fig. 7 using (14). *Top* $\widetilde{\psi}^j$ without scaling, *bottom* $\widetilde{\psi}^j$ with eight time zoom-in

irregularity of biorthogonal bases construction we show in Sect. 4.3, which prevents input $\widetilde{m_j}$ to be continuous in the first place. We also numerically verify that $m_j(\boldsymbol{\omega})$ and $\widetilde{m_j}(\boldsymbol{\omega})$ have the same phase, i.e. $m_j\overline{\widetilde{m_j}}(\boldsymbol{\omega}) \in \mathbb{R}$.

So far, we construct a set of $(m_j, \widetilde{m_j})_{j=0,\ldots,6}$ that satisfies (18) and (17), thus it can be used to construct biorthogonal wavelets based on (4) and (14). Figure 11 shows the dual wavelets $\widetilde{\psi}^j$ in (13) constructed using (14). Because of the regularity we impose on $\widetilde{m_j}$ and $\widetilde{m_0}'$, the dual wavelets are spatially localized and have good direction selection. The wavelets and scaling functions in (13) can be constructed using (4) similarly, but with much poorer regularity originated in m_j and m_0'.

Although using a different set of $\widetilde{m_j}$ as input paired with a carefully tweaked $\widetilde{m_0}'$ might improve the regularity of the dual wavelets $\widetilde{\psi}^j$, the intrinsic irregularity of the corresponding wavelets ψ^j shall remain.

7 Conclusion and Future Work

In this paper, we consider directional wavelet schemes on a dyadic quincunx sublattice and analyze their regularity. We show that filters in bi-orthogonal bases have the same discontinuity in the frequency domain as the orthonormal bases at the corners of $C_0 = [-\pi/2, \pi/2) \times [-\pi/2, \pi/2)$.

We propose a different approach to construct biorthogonal wavelets from our previous approach for the orthonormal bases construction [16]. The directional dual filters $\widetilde{m_j}$ are first designed such that they can be extended to a bi-orthogonal frame and the remaining filters are obtained by solving linear systems and a constrained quadratic optimization derived from the identity summation and shift cancellation conditions for a biorthogonal MRA. We show numerically that regularized dual wavelets $\widetilde{\psi}^j$ can be constructed, yet their corresponding wavelets ψ^j are still discontinuous in frequency domain, which is unavoidable according to our analysis.

We have looked at extensions of orthonormal bases in two different directions: tight frames (which are self-dual but redundant) with low redundancy and bi-orthogonal bases (which remain non-redundant but are no longer self-dual). In both cases we can gain some regularity. The extension of the biorthogonal bases to low-redundancy dual frame construction, which shall achieve at least the same regularity as low-redundancy tight frames but with more flexibility in the construction, is not studied here.

Acknowledgements This work is support by the NSF Grant 1516988.

Appendix 1: Proof of Theorem 1

Take the Fourier transform of both sides of (6), we have

$$\sum_{\boldsymbol{k}} \langle f, \phi_{\boldsymbol{k}} \rangle \hat{\phi}(\boldsymbol{\omega}) e^{-i\boldsymbol{\omega}^\top \boldsymbol{k}} = \sum_{\boldsymbol{k}} \langle f, \phi_{1,\boldsymbol{k}} \rangle e^{-i\boldsymbol{\omega}^\top \boldsymbol{D}\boldsymbol{k}} |\boldsymbol{D}|^{1/2} \hat{\phi}\left(\boldsymbol{D}^T \boldsymbol{\omega}\right) + \sum_{j=1}^{J} \sum_{\boldsymbol{k}} \left\langle f, \psi_{1,\boldsymbol{k}}^{j} \right\rangle e^{-i\boldsymbol{\omega}^\top \boldsymbol{Q}\boldsymbol{D}\boldsymbol{k}} |\boldsymbol{Q}\boldsymbol{D}|^{1/2} \hat{\phi}\left(\boldsymbol{D}^\top \boldsymbol{\omega}\right).$$

We use $\sum_{\boldsymbol{k}}$ for summation over $\mathbb{Z}^2$ without specifying the set $\mathbb{Z}^2$. Suppose m_j are trigonometric series

$$m_0(\boldsymbol{\omega}) = \sum_{\boldsymbol{k}} c_{\boldsymbol{k}} e^{-i\boldsymbol{\omega}^\top \boldsymbol{k}} \quad m_j(\boldsymbol{\omega}) = \sum_{\boldsymbol{k}} g_{\boldsymbol{k}} e^{-i\boldsymbol{\omega}^\top \boldsymbol{k}}, \quad j = 1, \ldots, J. \tag{33}$$

The first term on the right hand side can be represented by $\hat{\phi}(\boldsymbol{\omega})$ and $\langle f, \phi_k \rangle$ using (1) and (33).

$$\begin{aligned}
\text{the first term on R.H.S.} &= \sum_{\boldsymbol{k}} \langle f, \phi_{1,\boldsymbol{k}} \rangle e^{-i\boldsymbol{\omega}^\top \boldsymbol{D}\boldsymbol{k}} |\boldsymbol{D}|^{1/2} m_0(\boldsymbol{\omega}) \hat{\phi}(\boldsymbol{\omega}) \\
&= \sum_{\boldsymbol{k}} \left(\sum_{\boldsymbol{k}'} \langle f, \phi_{\boldsymbol{k}'} \rangle \overline{c_{\boldsymbol{k}'-\boldsymbol{D}\boldsymbol{k}}} |\boldsymbol{D}|^{1/2} \right) e^{-i\boldsymbol{\omega}^\top \boldsymbol{D}\boldsymbol{k}} |\boldsymbol{D}|^{1/2} m_0(\boldsymbol{\omega}) \hat{\phi}(\boldsymbol{\omega}) \\
&= \sum_{\boldsymbol{k}'} \langle f, \phi_{\boldsymbol{k}'} \rangle \left(|\boldsymbol{D}| \sum_{\boldsymbol{k}} \overline{c_{\boldsymbol{k}'-\boldsymbol{D}\boldsymbol{k}}} e^{i\boldsymbol{\omega}^\top (\boldsymbol{k}'-\boldsymbol{D}\boldsymbol{k})} \right) e^{-i\boldsymbol{\omega}^\top \boldsymbol{k}'} m_0(\boldsymbol{\omega}) \hat{\phi}(\boldsymbol{\omega}).
\end{aligned}$$

Let $\{\boldsymbol{\beta}\} \doteq \boldsymbol{D}\mathbb{Z}^2 + \boldsymbol{\beta}$ for $\boldsymbol{\beta} \in B$, *s.t.* $\bigcup_{\boldsymbol{\beta} \in B} \{\boldsymbol{\beta}\} = \mathbb{Z}^2$.[6] The sum over $\mathbb{Z}^2$ can then be written as a double sum $\sum_{\boldsymbol{\beta} \in B} \sum_{\boldsymbol{k}' \in \{\boldsymbol{\beta}\}}$,

[6] The choice of B is not unique and one choice is $\{(0, 0),\ (1, 0),\ (0, 1),\ (1, 1)\}$.

$$\sum_{\boldsymbol{\beta}\in B}\sum_{\boldsymbol{k}'\in\{\boldsymbol{\beta}\}}\langle f,\phi_{\boldsymbol{k}'}\rangle\sum_{\boldsymbol{k}}\overline{c_{\boldsymbol{k}'-\boldsymbol{D}\boldsymbol{k}}e^{i\boldsymbol{\omega}^\top(\boldsymbol{k}'-\boldsymbol{D}\boldsymbol{k})}}e^{-i\boldsymbol{\omega}^\top\boldsymbol{k}'}|\boldsymbol{D}|m_0(\boldsymbol{\omega})\hat{\phi}(\boldsymbol{\omega})$$

$$=\sum_{\boldsymbol{\beta}\in B}\sum_{\boldsymbol{k}'\in\{\boldsymbol{\beta}\}}\langle f,\phi_{\boldsymbol{k}'}\rangle\left(\sum_{\boldsymbol{k}\in\{\boldsymbol{\beta}\}}\overline{c_{\boldsymbol{k}}e^{i\boldsymbol{\omega}^\top\boldsymbol{k}}}\right)e^{-i\boldsymbol{\omega}^\top\boldsymbol{k}'}|\boldsymbol{D}|m_0(\boldsymbol{\omega})\hat{\phi}(\boldsymbol{\omega}).$$

Due to the identity $\sum_{\boldsymbol{\pi}\in\Gamma_0}e^{i\boldsymbol{\beta}^\top\boldsymbol{\pi}}=|\Gamma_0|\,\chi_{\boldsymbol{D}\mathbb{Z}^2}(\boldsymbol{\beta})$, the sum $\sum_{\boldsymbol{k}\in\{\boldsymbol{\beta}\}}c_{\boldsymbol{k}}e^{-i\boldsymbol{\omega}^\top\boldsymbol{k}}$ equals to a linear combination of m_0 with shifts in Γ_0,

$$\sum_{\boldsymbol{k}\in\{\boldsymbol{\beta}\}}c_{\boldsymbol{k}}e^{-i\boldsymbol{\omega}^\top\boldsymbol{k}}=\frac{1}{|\Gamma_0|}\sum_{\boldsymbol{\pi}\in\Gamma_0}m_0(\boldsymbol{\omega}+\boldsymbol{\pi})\,e^{i\boldsymbol{\beta}^\top\boldsymbol{\pi}}. \tag{34}$$

Substitute (34) into the previous expression and notice $|\Gamma_0|=|D|=4$, we have

$$\sum_{\boldsymbol{\beta}\in B}\sum_{\boldsymbol{k}'\in\{\boldsymbol{\beta}\}}\langle f,\phi_{\boldsymbol{k}'}\rangle\sum_{\boldsymbol{\pi}\in\Gamma_0}\overline{m_0}(\boldsymbol{\omega}+\boldsymbol{\pi})\,e^{-i\boldsymbol{\beta}^\top\boldsymbol{\pi}}\,e^{-i\boldsymbol{\omega}^\top\boldsymbol{k}'}m_0(\boldsymbol{\omega})\hat{\phi}(\boldsymbol{\omega}).$$

Since $e^{i\boldsymbol{\pi}^\top\boldsymbol{\beta}}=e^{i\boldsymbol{\pi}^\top\boldsymbol{k}'}$, for $\boldsymbol{k}'\in\{\boldsymbol{\beta}\}$, we can rewrite the double sum $\sum_{\boldsymbol{\beta}\in B}\sum_{\boldsymbol{k}'\in\{\boldsymbol{\beta}\}}$ back to a unit sum over $\mathbb{Z}^2$ as follows.

$$\sum_{\boldsymbol{k}'}\langle f,\phi_{\boldsymbol{k}'}\rangle e^{-i\boldsymbol{\omega}^\top\boldsymbol{k}'}\hat{\phi}(\boldsymbol{\omega})\left(\sum_{\boldsymbol{\pi}\in\Gamma_0}\overline{m_0}(\boldsymbol{\omega}+\boldsymbol{\pi})m_0(\boldsymbol{\omega})e^{-i\boldsymbol{\pi}^\top\boldsymbol{k}'}\right).$$

Similarly, the second term on the R.H.S. of (6) equals to

$$\sum_{j=1}^{J}\sum_{\boldsymbol{k}'}\langle f,\phi_{\boldsymbol{k}'}\rangle e^{-i\boldsymbol{\omega}^\top\boldsymbol{k}'}\hat{\phi}(\boldsymbol{\omega})\left(\sum_{\boldsymbol{\pi}\in\Gamma_1}\overline{m_j}(\boldsymbol{\omega}+\boldsymbol{\pi})m_j(\boldsymbol{\omega})e^{-i\boldsymbol{\pi}^\top\boldsymbol{k}'}\right)$$

based on the following equality analogous to (34)

$$\sum_{\boldsymbol{k}\in\{\boldsymbol{\alpha}\}}g_{\boldsymbol{k}'}e^{-i\boldsymbol{\omega}^\top\boldsymbol{k}}=\frac{1}{|\Gamma_1|}\sum_{\boldsymbol{\pi}\in\Gamma_1}m_j(\boldsymbol{\omega}+\boldsymbol{\pi})e^{i\boldsymbol{\alpha}^\top\boldsymbol{\pi}}, \tag{35}$$

where $\{\boldsymbol{\alpha}\}\doteq\boldsymbol{Q}\boldsymbol{D}\mathbb{Z}^2+\boldsymbol{\alpha}$ for $\boldsymbol{\alpha}\in A$, $s.t.$ $\bigcup_{\boldsymbol{\alpha}\in A}\{\boldsymbol{\alpha}\}=\mathbb{Z}^2$. (For Theorem 3 on frame construction, the summation of shifts $\boldsymbol{\pi}$ is over Γ_0 instead of Γ_1.) Combining the two terms on the R.H.S. of (6), and compare the coefficients of $\langle f,\phi_{\boldsymbol{k}'}\rangle e^{-i\boldsymbol{\omega}^\top\boldsymbol{k}'}\hat{\phi}(\boldsymbol{\omega})$ on both sides, the perfect reconstruction condition is then equivalent to for all $\boldsymbol{k}'$,

$$\sum_{\boldsymbol{\pi}\in\Gamma_0}e^{-i\boldsymbol{\pi}^\top\boldsymbol{k}'}\overline{m_0}(\boldsymbol{\omega}+\boldsymbol{\pi})m_0(\boldsymbol{\omega})+\sum_{j}\sum_{\boldsymbol{\pi}\in\Gamma_1}e^{-i\boldsymbol{\pi}^\top\boldsymbol{k}'}\overline{m_j}(\boldsymbol{\omega}+\boldsymbol{\pi})m_j(\boldsymbol{\omega})=1.$$

This is equivalent to

$$|m_0(\boldsymbol{\omega})|^2 + \sum_j |m_j(\boldsymbol{\omega})|^2 = 1$$

and

$$\sum_{j=0}^{J} \overline{m_j}(\boldsymbol{\omega}+\boldsymbol{\pi})m_j(\boldsymbol{\omega}) = 0,\ \boldsymbol{\pi} \in \Gamma_0\backslash\{\mathbf{0}\}$$
$$\sum_{j=1}^{J} \overline{m_j}(\boldsymbol{\omega}+\boldsymbol{\pi})m_j(\boldsymbol{\omega}) = 0,\ \boldsymbol{\pi} \in \Gamma_1\backslash\Gamma_0$$

□

Remark If we have a shift $\boldsymbol{k}_0$ in the down-sample scheme for ϕ_1, i.e. $\boldsymbol{D}\mathbb{Z}^2 - \boldsymbol{k}_0$ instead of $\boldsymbol{D}\mathbb{Z}^2$, so that we obtain coefficient of $\tilde{\phi}_{1,\boldsymbol{k}} = \phi_{1,\boldsymbol{k}+\boldsymbol{k}_0}$ instead of $\phi_{1,\boldsymbol{k}}$, and $\tilde{\phi}_1(\boldsymbol{x}) = \phi_1(\boldsymbol{x}-\boldsymbol{k}_0) = |\boldsymbol{D}|^{1/2}\sum_{\boldsymbol{k}} c_{\boldsymbol{k}}\phi(\boldsymbol{x}-\boldsymbol{k}-\boldsymbol{k}_0) = |\boldsymbol{D}|^{1/2}\sum_{\boldsymbol{k}} c_{\boldsymbol{k}-\boldsymbol{k}_0}\phi(\boldsymbol{x}-\boldsymbol{k})$. This change of down-sample scheme results in an extra phase term $e^{-i\boldsymbol{\omega}^\top \boldsymbol{k}_0}$ in m_0. Similarly, if we downsample ψ_1^j on a shifted sub-lattice $\boldsymbol{Q}\boldsymbol{D}\mathbb{Z}^2 - \boldsymbol{k}_j$, we then have an extra phase $e^{i\boldsymbol{\pi}^\top \boldsymbol{k}_j}$ before $\overline{m_j}(\boldsymbol{\omega}+\boldsymbol{\pi})m_j(\boldsymbol{\omega})$ in shift cancellation condition. This provides additional freedom in the construction yet it is not substantial. Here, we use the down-sample scheme without translation.

Appendix 2: Proof of Lemmas and Propositions for Biorthogonal Schemes

Discontinuity of $\widetilde{m_j}(\boldsymbol{\omega})$

Lemma 9.1 *Define* $d_{i,j}(\boldsymbol{\omega}) = \det([\widetilde{\mathbf{m}}^{k_1}(\boldsymbol{\omega})^\top, \ldots, \widetilde{\mathbf{m}}^{k_6}(\boldsymbol{\omega})^\top])$, *where* $0 \le k_1 < \cdots < k_6 \le 7$, *s.t.* $k_l \ne i, j$. (18) *is solvable for all* $\boldsymbol{\omega}$ *if and only if*

$$\mathfrak{D}(\boldsymbol{\omega})\begin{bmatrix}\overline{\widetilde{m_0}}(\boldsymbol{\omega})\\ \overline{\widetilde{m_0}}(\boldsymbol{\omega}+\boldsymbol{\pi}_2)\\ \overline{\widetilde{m_0}}(\boldsymbol{\omega}+\boldsymbol{\pi}_4)\\ \overline{\widetilde{m_0}}(\boldsymbol{\omega}+\boldsymbol{\pi}_6)\end{bmatrix} \doteq \begin{bmatrix}0 & d_{0,2} & d_{0,4} & d_{0,6}\\ -d_{0,2} & 0 & d_{2,4} & d_{2,6}\\ -d_{0,4} & -d_{2,4} & 0 & d_{4,6}\\ -d_{0,6} & -d_{2,6} & -d_{4,6} & 0\end{bmatrix}\begin{bmatrix}\overline{\widetilde{m_0}}(\boldsymbol{\omega})\\ \overline{\widetilde{m_0}}(\boldsymbol{\omega}+\boldsymbol{\pi}_2)\\ \overline{\widetilde{m_0}}(\boldsymbol{\omega}+\boldsymbol{\pi}_4)\\ \overline{\widetilde{m_0}}(\boldsymbol{\omega}+\boldsymbol{\pi}_6)\end{bmatrix} = \begin{bmatrix}0\\0\\0\\0\end{bmatrix}. \tag{36}$$

Proof By Lemmas 4.1 and 4.2, $\widetilde{\mathbf{M}}[\widehat{k},:]$, $k = 0, 2, 4, 6$ are singular, The singularity condition on $\widetilde{\mathbf{M}}[\widehat{0},:](\boldsymbol{\omega})$ can be rewritten as follows,

$$\begin{aligned}0 &= \det(\widetilde{\mathbf{M}}[\widehat{0},:])\\ &= \overline{\widetilde{m_0}}(\boldsymbol{\omega}+\boldsymbol{\pi}_2)\cdot\det(\widetilde{\mathbf{M}}^{\square}[\widehat{2},:])\\ &\qquad + \overline{\widetilde{m_0}}(\boldsymbol{\omega}+\boldsymbol{\pi}_4)\cdot\det(\widetilde{\mathbf{M}}^{\square}[\widehat{4},:]) + \overline{\widetilde{m_0}}(\boldsymbol{\omega}+\boldsymbol{\pi}_6)\cdot\det(\widetilde{\mathbf{M}}^{\square}[\widehat{6},:])\\ &= 0\cdot\overline{\widetilde{m_0}}(\boldsymbol{\omega}) + d_{0,2}\cdot\overline{\widetilde{m_0}}(\boldsymbol{\omega}+\boldsymbol{\pi}_2)\\ &\qquad + d_{0,4}\cdot\overline{\widetilde{m_0}}(\boldsymbol{\omega}+\boldsymbol{\pi}_4) + d_{0,6}\cdot\overline{\widetilde{m_0}}(\boldsymbol{\omega}+\boldsymbol{\pi}_6)\end{aligned} \tag{37}$$

Similarly, the second to fourth equations can be obtained by rewriting the singularity condition on $\widetilde{\mathbf{M}}[\widehat{2},:]$, $\widetilde{\mathbf{M}}[\widehat{4},:]$ and $\widetilde{\mathbf{M}}[\widehat{6},:]$ respectively. $\square$

The identity constraint (17) on m_0 and the singularity condition (36) together imply the following proposition,

Proposition 9.2 *Given $\widetilde{m_i}$, $i=1,\ldots,6$, (17) has no solution for $\widetilde{m_0}$, if there exists $\boldsymbol{\omega}$, s.t. $[m_0(\boldsymbol{\omega}), m_0(\boldsymbol{\omega}+\boldsymbol{\pi}_2), m_0(\boldsymbol{\omega}+\boldsymbol{\pi}_4), m_0(\boldsymbol{\omega}+\boldsymbol{\pi}_6)]$ is a linear combination of the rows of $\mathfrak{D}(\boldsymbol{\omega})$.*

Proof of Lemma 4.3:
Lemma 4.3 *If $\boldsymbol{\omega} \in S_\rho$ such that (17) holds and $\widetilde{\mathbf{M}}[\widehat{0},:](\boldsymbol{\omega})$ is singular, then $rank(\widetilde{\mathbf{m}}^1, \widetilde{\mathbf{m}}^7) = 1$ and $rank(\widetilde{\mathbf{m}}^3, \widetilde{\mathbf{m}}^5) = 2$ or $rank(\widetilde{\mathbf{m}}^3, \widetilde{\mathbf{m}}^5) = 1$ and $rank(\widetilde{\mathbf{m}}^1, \widetilde{\mathbf{m}}^7) = 2$.*

Proof When ρ is small enough, due to the concentration property, $\widetilde{m_i}(\boldsymbol{\omega})$ is zero on all but a few sets $S_\rho + \boldsymbol{\pi}_j$ (see Fig. 4 for reference of S_ρ and its shifts), thus $\widetilde{\mathbf{m}}^i(\boldsymbol{\omega})$ is sparse on S_ρ and $\widetilde{\mathbf{M}}[:,\widehat{0}]$ takes the following form

$$\widetilde{\mathbf{M}}[:,\widehat{0}](\boldsymbol{\omega}) = \begin{bmatrix} \widetilde{\mathbf{m}}^0 \\ \widetilde{\mathbf{m}}^1 \\ \widetilde{\mathbf{m}}^2 \\ \widetilde{\mathbf{m}}^3 \\ \widetilde{\mathbf{m}}^4 \\ \widetilde{\mathbf{m}}^5 \\ \widetilde{\mathbf{m}}^6 \\ \widetilde{\mathbf{m}}^7 \end{bmatrix} = \begin{bmatrix} 0 & 0 & 0 & 0 & 0 & 0 \\ * & 0 & 0 & 0 & 0 & * \\ 0 & 0 & 0 & * & * & 0 \\ 0 & 0 & * & * & 0 & 0 \\ 0 & * & * & 0 & 0 & 0 \\ 0 & 0 & * & * & 0 & 0 \\ * & 0 & * & * & 0 & * \\ * & 0 & 0 & 0 & 0 & * \end{bmatrix} \tag{38}$$

where $*$ denote possible non-zero entries. We make the following observation of $\widetilde{\mathbf{m}}^i$:

(i) $\widetilde{\mathbf{m}}^0$ is a zero vector
(ii) $\widetilde{\mathbf{m}}^2$ and $\widetilde{\mathbf{m}}^4$ are linearly independent of each other and the rest of $\widetilde{\mathbf{m}}^i$
(iii) $span\{\widetilde{\mathbf{m}}^1, \widetilde{\mathbf{m}}^7\} \perp span\{\widetilde{\mathbf{m}}^3, \widetilde{\mathbf{m}}^5\}$ and $rank(\widetilde{\mathbf{m}}^1, \widetilde{\mathbf{m}}^7) \le 2$, $rank(\widetilde{\mathbf{m}}^3, \widetilde{\mathbf{m}}^5) \le 2$
(iv) $span\{\widetilde{\mathbf{m}}^1, \widetilde{\mathbf{m}}^7, \widetilde{\mathbf{m}}^3, \widetilde{\mathbf{m}}^5, \widetilde{\mathbf{m}}^6\} \le 4$

Since $m_0(\boldsymbol{\omega}) \ne 0$ on S_ρ, (22) then implies that $\det(\widetilde{\mathbf{M}}^{\square}[\widehat{k_{\boldsymbol{\omega}}},:]) \ne 0$. Therefore, $\widetilde{\mathbf{M}}^{\square}$ is full rank, or equivalently, $rank(\widetilde{\mathbf{M}}[:,\widehat{0}]) = 6$. It follows from (ii) and (iv) that $rank(\widetilde{\mathbf{m}}^1, \widetilde{\mathbf{m}}^6, \widetilde{\mathbf{m}}^7, \widetilde{\mathbf{m}}^3, \widetilde{\mathbf{m}}^5) = 4$.
On the other hand, (ii) and (iv) imply that

$$rank\left(\widetilde{\mathbf{M}}^{\square}(\boldsymbol{\omega}+\boldsymbol{\pi}_2)\right) = rank\left(\widetilde{\mathbf{m}}^0, \widetilde{\mathbf{m}}^4, \widetilde{\mathbf{m}}^6, \widetilde{\mathbf{m}}^1, \widetilde{\mathbf{m}}^3, \widetilde{\mathbf{m}}^5, \widetilde{\mathbf{m}}^7\right) = 5$$

and likewise

$$rank\left(\widetilde{\mathbf{M}}^{\square}(\boldsymbol{\omega}+\boldsymbol{\pi}_4)\right) = rank\left(\widetilde{\mathbf{m}}^0, \widetilde{\mathbf{m}}^2, \widetilde{\mathbf{m}}^6, \widetilde{\mathbf{m}}^1, \widetilde{\mathbf{m}}^3, \widetilde{\mathbf{m}}^5, \widetilde{\mathbf{m}}^7\right) = 5.$$

Therefore, $\det(\widetilde{\mathbf{M}}^{\square}(\boldsymbol{\omega}+\boldsymbol{\pi}_2)) = \det(\widetilde{\mathbf{M}}^{\square}(\boldsymbol{\omega}+\boldsymbol{\pi}_4)) = 0$ and (22) implies $m_0(\boldsymbol{\omega}+\boldsymbol{\pi}_2) = m_0(\boldsymbol{\omega}+\boldsymbol{\pi}_4) = 0$. If $\widetilde{\mathbf{m}}^1$ and $\widetilde{\mathbf{m}}^7$ are linearly independent and so are $\widetilde{\mathbf{m}}^3$ and $\widetilde{\mathbf{m}}^5$, then

$$rank\left(\widetilde{\mathbf{M}}^{\square}(\boldsymbol{\omega}+\boldsymbol{\pi}_6)\right) = rank\left(\widetilde{\mathbf{m}}^2, \widetilde{\mathbf{m}}^4, \widetilde{\mathbf{m}}^1, \widetilde{\mathbf{m}}^3, \widetilde{\mathbf{m}}^5, \widetilde{\mathbf{m}}^7\right) = 6,$$

hence $m_0(\boldsymbol{\omega}+\boldsymbol{\pi}_6) \neq 0$. Therefore,

$$[m_0(\boldsymbol{\omega}), m_0(\boldsymbol{\omega}+\boldsymbol{\pi}_2), m_0(\boldsymbol{\omega}+\boldsymbol{\pi}_4), m_0(\boldsymbol{\omega}+\boldsymbol{\pi}_6)] = [*, 0, 0, *].$$

In addition, $d_{i,j} = 0$, $\forall(i, j)$ except $(0, 6)$, so in (36)

$$\mathfrak{D}(\boldsymbol{\omega}) = [d_{0,6}, 0, 0, 0]^{\top}[0, 0, 0, 1] + [0, 0, 0, d_{0,6}]^{\top}[-1, 0, 0, 0].$$

By Proposition 9.2, (17) cannot be satisfied, hence $rank(\widetilde{\mathbf{m}}^1, \widetilde{\mathbf{m}}^7) \leq 1$ or $rank(\widetilde{\mathbf{m}}^3, \widetilde{\mathbf{m}}^5) \leq 1$.

As $rank(\widetilde{\mathbf{m}}^1, \widetilde{\mathbf{m}}^6, \widetilde{\mathbf{m}}^7, \widetilde{\mathbf{m}}^3, \widetilde{\mathbf{m}}^5) = 4$, we must have $rank(\widetilde{\mathbf{m}}^1, \widetilde{\mathbf{m}}^7) = 1$ and $rank(\widetilde{\mathbf{m}}^3, \widetilde{\mathbf{m}}^5) = 2$ or $rank(\widetilde{\mathbf{m}}^3, \widetilde{\mathbf{m}}^5) = 1$ and $rank(\widetilde{\mathbf{m}}^1, \widetilde{\mathbf{m}}^7) = 2$. □

Lemma 9.3 *Let $\widetilde{S_\rho} = S_\rho \cap \{\boldsymbol{\omega} : rank(\widetilde{\mathbf{m}}^3(\boldsymbol{\omega}), \widetilde{\mathbf{m}}^5(\boldsymbol{\omega})) = 1\}$, if $\widetilde{m_3}(\boldsymbol{\omega})$ and $\widetilde{m_4}(\boldsymbol{\omega})$ concentrate in T_3 and T_4 respectively, then $|\widetilde{S_\rho}| = 0$.*

Proof Let $\widetilde{S_\rho} + \boldsymbol{\pi}_3 = \{\boldsymbol{\omega}+\boldsymbol{\pi}_3, \boldsymbol{\omega} \in \widetilde{S_\rho}\}$ and Ω' be the set symmetric to a set $\Omega \subset S_0$ with respect to the diagonal $\omega_1 = -\omega_2$. If $|\widetilde{S_\rho}| > 0$, by the concentration of $\widetilde{m_3}(\boldsymbol{\omega})$ in T_3, for any $\Omega \subset \widetilde{S_\rho} + \boldsymbol{\pi}_3 \subset T_3$ s.t. $|\Omega| > 0$, $\int_\Omega |\widetilde{m_3}| > \int_{\Omega'} |\widetilde{m_3}|$. Due to the symmetry between $|\widetilde{m_3}|$ and $|\widetilde{m_4}|$ defined in (24), $\int_{\Omega'} |\widetilde{m_3}| = \int_\Omega |\widetilde{m_4}|$. Therefore, $\int_\Omega |\widetilde{m_3}| > \int_\Omega |\widetilde{m_4}|$ which implies that $|\widetilde{m_3}(\boldsymbol{\omega})| > |\widetilde{m_4}(\boldsymbol{\omega})|$ *a.e.* on $\widetilde{S_\rho}+\boldsymbol{\pi}_3$ or equivalently $|\widetilde{m_3}(\boldsymbol{\omega}+\boldsymbol{\pi}_3)| > |\widetilde{m_4}(\boldsymbol{\omega}+\boldsymbol{\pi}_3)|$ *a.e.* on $\widetilde{S_\rho}$. Similarly, we have $|\widetilde{m_4}(\boldsymbol{\omega}+\boldsymbol{\pi}_5)| > |\widetilde{m_3}(\boldsymbol{\omega}+\boldsymbol{\pi}_5)|$ *a.e.* on $\widetilde{S_\rho}$ following the same analysis on $\widetilde{S_\rho}+\boldsymbol{\pi}_5 \subset T_4$. On the other hand, $rank(\widetilde{\mathbf{m}}^3(\boldsymbol{\omega}), \widetilde{\mathbf{m}}^5(\boldsymbol{\omega})) = 1$ on $\widetilde{S_\rho}$, hence $\widetilde{m_3}(\boldsymbol{\omega}+\boldsymbol{\pi}_3)\widetilde{m_4}(\boldsymbol{\omega}+\boldsymbol{\pi}_5) = \widetilde{m_3}(\boldsymbol{\omega}+\boldsymbol{\pi}_5)\widetilde{m_4}(\boldsymbol{\omega}+\boldsymbol{\pi}_3)$, which contradicts the previous two inequalities. □

Lemma 9.4 *If $\widetilde{m_1}(\boldsymbol{\omega})$ (respectively, $\widetilde{m_6}(\boldsymbol{\omega})$) concentrates in T_1 (respectively, T_6), then $|\widetilde{m_6}(\boldsymbol{\omega})| > |\widetilde{m_1}(\boldsymbol{\omega})|$ a.e. on $T_6 \bigcap supp(\widetilde{m_6})$ (respectively, $|\widetilde{m_1}(\boldsymbol{\omega})| > |\widetilde{m_6}(\boldsymbol{\omega})|$ a.e. on $T_1 \bigcap supp(\widetilde{m_1})$).*

Proof Let $B_6 = \{\boldsymbol{\omega} : |\widetilde{m_6}(\boldsymbol{\omega})| \leq |\widetilde{m_1}(\boldsymbol{\omega})|\} \bigcap T_6 \bigcap supp(\widetilde{m_1})$ and B_1 be the set symmetric to B_6 with respect to $\omega_1 = \omega_2$ and suppose $|B_6| > 0$, then $\int_{B_6} |\widetilde{m_6}(\boldsymbol{\omega})| \leq \int_{B_6} |\widetilde{m_1}(\boldsymbol{\omega})|$. On the other hand, since $\widetilde{m_1}(\boldsymbol{\omega})$ concentrates in T_1, we know $\int_{B_1} |\widetilde{m_1}(\boldsymbol{\omega})| > \int_{B_6} |\widetilde{m_1}(\boldsymbol{\omega})|$. Moreover, due to the symmetry of $\widetilde{m_1}(\boldsymbol{\omega}), \widetilde{m_6}(\boldsymbol{\omega})$ and B_1, B_6, $\int_{B_1} |\widetilde{m_1}(\boldsymbol{\omega})| = \int_{B_6} |\widetilde{m_6}(\boldsymbol{\omega})|$, hence $\int_{B_6} |\widetilde{m_1}(\boldsymbol{\omega})| \geq \int_{B_6} |\widetilde{m_6}(\boldsymbol{\omega})| = \int_{B_1} |\widetilde{m_1}(\boldsymbol{\omega})|$ which results in contradiction. □

Proposition 9.5 *If $\widetilde{m_0}(\boldsymbol{\omega})$, $\widetilde{m_1}(\boldsymbol{\omega})$ and $\widetilde{m_6}(\boldsymbol{\omega})$ concentrate in C_0, T_1 and T_6 respectively, then $\widetilde{m_6}(\boldsymbol{\omega}) = 0$ a.e. on $S'_\rho + \boldsymbol{\pi}_1$, where $S'_\rho = S_\rho \bigcap \{\omega_1 < \omega_2\}$.*

Proof By Lemma 9.4, the concentration of $\widetilde{m_1}(\boldsymbol{\omega})$ in T_1 implies that $|\widetilde{m_6}(\boldsymbol{\omega}+\boldsymbol{\pi}_1)| > |\widetilde{m_1}(\boldsymbol{\omega}+\boldsymbol{\pi}_1)|$ a.e. on $S'_\rho \cap \{\boldsymbol{\omega},\ \widetilde{m_6}(\boldsymbol{\omega}+\boldsymbol{\pi}_1) \neq 0\}$. Similarly, the concentration of $\widetilde{m_6}(\boldsymbol{\omega})$ in T_6 implies that $|\widetilde{m_1}(\boldsymbol{\omega}+\boldsymbol{\pi}_7)| > |\widetilde{m_6}(\boldsymbol{\omega}+\boldsymbol{\pi}_7)|$ a.e. on $S'_\rho \cap \{\boldsymbol{\omega},\ \widetilde{m_1}(\boldsymbol{\omega}+\boldsymbol{\pi}_7) \neq 0\}$. Therefore, $|\widetilde{m_1}(\boldsymbol{\omega}+\boldsymbol{\pi}_7)\widetilde{m_6}(\boldsymbol{\omega}+\boldsymbol{\pi}_1)| > |\widetilde{m_1}(\boldsymbol{\omega}+\boldsymbol{\pi}_1)\widetilde{m_6}(\boldsymbol{\omega}+\boldsymbol{\pi}_7)|$ a.e. on $S'_\rho \cap \{\boldsymbol{\omega},\ \widetilde{m_6}(\boldsymbol{\omega}+\boldsymbol{\pi}_1) \neq 0\} \cap \{\boldsymbol{\omega},\ \widetilde{m_1}(\boldsymbol{\omega}+\boldsymbol{\pi}_7) \neq 0\}$.

On the other hand, Lemma 4.3 implies that for a.e. $\boldsymbol{\omega} \in S'_\rho, rank(\widetilde{\mathbf{m}}^1(\boldsymbol{\omega}),\ \widetilde{\mathbf{m}}^7(\boldsymbol{\omega})) = 1$, hence $\widetilde{m_1}(\boldsymbol{\omega}+\boldsymbol{\pi}_7)\widetilde{m_6}(\boldsymbol{\omega}+\boldsymbol{\pi}_1) = \widetilde{m_1}(\boldsymbol{\omega}+\boldsymbol{\pi}_1)\widetilde{m_6}(\boldsymbol{\omega}+\boldsymbol{\pi}_7)$. Together with the previous result, this forces $|S'_\rho \cap \{\boldsymbol{\omega},\ \widetilde{m_6}(\boldsymbol{\omega}+\boldsymbol{\pi}_1) \neq 0\} \cap \{\boldsymbol{\omega},\ \widetilde{m_1}(\boldsymbol{\omega}+\boldsymbol{\pi}_7) \neq 0\}| = 0$.

The concentration of $\widetilde{m_0}(\boldsymbol{\omega}), \widetilde{m_1}(\boldsymbol{\omega})$ and $\widetilde{m_6}(\boldsymbol{\omega})$ in C_0, T_1 and T_6 implies that $\widetilde{m_1}(\boldsymbol{\omega}+\boldsymbol{\pi}_7) \neq 0$ on S'_ρ, since $\boldsymbol{\omega}+\boldsymbol{\pi}_7 \notin C_0 \cup T_6$, $\forall \boldsymbol{\omega} \in S'_\rho$ and neither $\widetilde{m_6}$ or $\widetilde{m_0}$ can dominate at $\boldsymbol{\omega}+\boldsymbol{\pi}_7$. Therefore, $S'_\rho \cap \{\boldsymbol{\omega}, \widetilde{m_1}(\boldsymbol{\omega}+\boldsymbol{\pi}_7) \neq 0\} = S'_\rho$ which implies $|S'_\rho \cap \{\boldsymbol{\omega},\ \widetilde{m_6}(\boldsymbol{\omega}+\boldsymbol{\pi}_1) \neq 0\}| = 0$, i.e. $\widetilde{m_6}(\boldsymbol{\omega}) = 0$ a.e. on $S'_\rho + \boldsymbol{\pi}_1$. □

Design of Input $\widetilde{m_j}(\omega)$

Proof of Lemma 5.1:
Lemma 5.1 If there exist $\boldsymbol{\omega} \in D_1 := \{\omega_1 = \omega_2,\ \omega_1 \in (-\frac{\pi}{2}, 0)\}$, $s.t. |m_0(\boldsymbol{\omega})| \neq 0$, then $(\boldsymbol{\eta}_1 - \boldsymbol{\eta}_6)^\top(\boldsymbol{\pi}_6 - \boldsymbol{\pi}_7) \neq 0 (\mathrm{mod}\, 2\pi)$.

Proof As $\widetilde{m_1}(\boldsymbol{\omega})$ and $\widetilde{m_6}(\boldsymbol{\omega})$ concentrate in T_1 and T_6 respectively, $\widetilde{m_1}(\boldsymbol{\omega}+\boldsymbol{\pi}_i) = 0$ and $\widetilde{m_6}(\boldsymbol{\omega}+\boldsymbol{\pi}_i) = 0$, $i = 1, \ldots, 5$. Due to symmetry, $|\widetilde{m_1}(\boldsymbol{\omega})| = |\widetilde{m_6}(\boldsymbol{\omega})|$ on $\{\omega_1 = \omega_2\}$. Let $A = |\widetilde{m_1}(\boldsymbol{\omega}+\boldsymbol{\pi}_7)| = |\widetilde{m_6}(\boldsymbol{\omega}+\boldsymbol{\pi}_7)|$ and $B = |\widetilde{m_1}(\boldsymbol{\omega}+\boldsymbol{\pi}_6)| = |\widetilde{m_6}(\boldsymbol{\omega}+\boldsymbol{\pi}_6)|$, then the first and the last columns of $\widetilde{\mathbf{M}}^\square$ are

$$\widetilde{\mathbf{M}}^\square[:, 1] = \begin{bmatrix} 0 \\ \vdots \\ 0 \\ Ae^{i\boldsymbol{\eta}_1^\top(\boldsymbol{\omega}+\boldsymbol{\pi}_6)} \\ Be^{i\boldsymbol{\eta}_1^\top(\boldsymbol{\omega}+\boldsymbol{\pi}_7)} \end{bmatrix} \quad \text{and} \quad \widetilde{\mathbf{M}}^\square[:, 6] = \begin{bmatrix} 0 \\ \vdots \\ 0 \\ Ae^{i\boldsymbol{\eta}_6^\top(\boldsymbol{\omega}+\boldsymbol{\pi}_6)} \\ Be^{i\boldsymbol{\eta}_6^\top(\boldsymbol{\omega}+\boldsymbol{\pi}_7)} \end{bmatrix}.$$

By (22), if $m_0(\boldsymbol{\omega}) > 0$, $\boldsymbol{\omega} \in D_1$ then $\widetilde{\mathbf{M}}^\square(\boldsymbol{\omega})$ is full rank, hence its columns are linearly independent. In particular, $\widetilde{\mathbf{M}}^\square[:, 1]$ and $\widetilde{\mathbf{M}}^\square[:, 6]$ are linearly independent, which implies that $e^{i(\boldsymbol{\eta}_1^\top\boldsymbol{\pi}_6+\boldsymbol{\eta}_6^\top\boldsymbol{\pi}_7)} \neq e^{i(\boldsymbol{\eta}_6^\top\boldsymbol{\pi}_6+\boldsymbol{\eta}_1^\top\boldsymbol{\pi}_7)}$ or equivalently $(\boldsymbol{\eta}_1 - \boldsymbol{\eta}_6)^\top(\boldsymbol{\pi}_6 - \boldsymbol{\pi}_7) \neq 0(\mathrm{mod} 2\pi)$. □

Proof of Proposition 5.2
Proposition 5.2 If $\widetilde{m_0}(\mathbf{0}) \neq 0$, then $\boldsymbol{\pi}_1^\top(\boldsymbol{\eta}_1 - \boldsymbol{\eta}_6) \neq \pi(\mathrm{mod}\, 2\pi)$ or $\boldsymbol{\pi}_3^\top(\boldsymbol{\eta}_3 - \boldsymbol{\eta}_4) \neq \pi(\mathrm{mod}\, 2\pi)$.

Proof Since $\widetilde{m_0}(\mathbf{0}) \neq 0$, as shown in Lemma 4.3, at $\boldsymbol{\omega} = \mathbf{0}\, rank(\widetilde{\mathbf{m}}^1, \widetilde{\mathbf{m}}^6, \widetilde{\mathbf{m}}^7, \widetilde{\mathbf{m}}^3, \widetilde{\mathbf{m}}^5) = 4$. This is equivalent to the matrix $\boldsymbol{A}$ defined in (39) to be full rank.

$$\boldsymbol{A} = \begin{bmatrix} \widetilde{m_1}(\boldsymbol{\pi}_6) & \widetilde{m_6}(\boldsymbol{\pi}_6) & \widetilde{m_3}(\boldsymbol{\pi}_6) & \widetilde{m_4}(\boldsymbol{\pi}_6) \\ \widetilde{m_1}(\boldsymbol{\pi}_1) & \widetilde{m_6}(\boldsymbol{\pi}_1) & 0 & 0 \\ \widetilde{m_1}(\boldsymbol{\pi}_7) & \widetilde{m_6}(\boldsymbol{\pi}_7) & 0 & 0 \\ 0 & 0 & \widetilde{m_3}(\boldsymbol{\pi}_3) & \widetilde{m_4}(\boldsymbol{\pi}_3) \\ 0 & 0 & \widetilde{m_3}(\boldsymbol{\pi}_5) & \widetilde{m_4}(\boldsymbol{\pi}_5) \end{bmatrix} \tag{39}$$

Let $|\widetilde{m_1}(\boldsymbol{\pi}_1)| = a$, $|\widetilde{m_1}(\boldsymbol{\pi}_6)| = b$. Due to the symmetry of $\widetilde{m_j}(\boldsymbol{\omega})$, $|\widetilde{m_1}(\boldsymbol{\pi}_1)| = |\widetilde{m_1}(\boldsymbol{\pi}_7)| = |\widetilde{m_6}(\boldsymbol{\pi}_1)| = |\widetilde{m_6}(\boldsymbol{\pi}_7)| = |\widetilde{m_3}(\boldsymbol{\pi}_3)| = |\widetilde{m_3}(\boldsymbol{\pi}_5)| = |\widetilde{m_4}(\boldsymbol{\pi}_3)| = |\widetilde{m_4}(\boldsymbol{\pi}_5)|$ and $|\widetilde{m_1}(\boldsymbol{\pi}_6)| = |\widetilde{m_6}(\boldsymbol{\pi}_6)| = |\widetilde{m_3}(\boldsymbol{\pi}_6)| = |\widetilde{m_4}(\boldsymbol{\pi}_6)|$. Rewrite $\boldsymbol{A}$ as follows,

$$\boldsymbol{A} = \begin{bmatrix} be^{-i\boldsymbol{\pi}_6^\top \boldsymbol{\eta}_1} & be^{-i\boldsymbol{\pi}_6^\top \boldsymbol{\eta}_6} & be^{-i\boldsymbol{\pi}_6^\top \boldsymbol{\eta}_3} & be^{-i\boldsymbol{\pi}_6^\top \boldsymbol{\eta}_4} \\ ae^{-i\boldsymbol{\pi}_1^\top \boldsymbol{\eta}_1} & ae^{-i\boldsymbol{\pi}_1^\top \boldsymbol{\eta}_6} & 0 & 0 \\ ae^{i\boldsymbol{\pi}_1^\top \boldsymbol{\eta}_1} & ae^{i\boldsymbol{\pi}_1^\top \boldsymbol{\eta}_6} & 0 & 0 \\ 0 & 0 & ae^{-i\boldsymbol{\pi}_3^\top \boldsymbol{\eta}_3} & ae^{-i\boldsymbol{\pi}_3^\top \boldsymbol{\eta}_4} \\ 0 & 0 & ae^{i\boldsymbol{\pi}_3^\top \boldsymbol{\eta}_3} & ae^{i\boldsymbol{\pi}_3^\top \boldsymbol{\eta}_4} \end{bmatrix}$$

The product of singular values of $\boldsymbol{A}$ is

$$\sqrt{\det(\boldsymbol{A}^*\boldsymbol{A})} = 4a^3\sqrt{a^2K_1^2K_2^2 + b^2(Q_1K_2^2 + Q_2K_1^2)}, \tag{40}$$

where $Q_1 = 1 - \cos(\boldsymbol{\pi}_6^\top(\boldsymbol{\eta}_1 - \boldsymbol{\eta}_6))\cos(\boldsymbol{\pi}_1^\top(\boldsymbol{\eta}_1 - \boldsymbol{\eta}_6))$, $Q_2 = 1 - \cos(\boldsymbol{\pi}_6^\top(\boldsymbol{\eta}_3 - \boldsymbol{\eta}_4))\cos(\boldsymbol{\pi}_3^\top(\boldsymbol{\eta}_3 - \boldsymbol{\eta}_4))$, $K_1 = \sin(\boldsymbol{\pi}_1^\top(\boldsymbol{\eta}_1 - \boldsymbol{\eta}_6))$, $K_2 = \sin(\boldsymbol{\pi}_3^\top(\boldsymbol{\eta}_3 - \boldsymbol{\eta}_4))$. If $\boldsymbol{\pi}_1^\top(\boldsymbol{\eta}_1 - \boldsymbol{\eta}_6) = \boldsymbol{\pi}_3^\top(\boldsymbol{\eta}_3 - \boldsymbol{\eta}_4) = \pi(mod\, 2\pi)$, then $K_1 = K_2 = 0$ and $\boldsymbol{A}$ becomes singular. □

Solving (18) and (17) for $\boldsymbol{m_0}$, $\widetilde{\boldsymbol{m_0}}$ and $\boldsymbol{m_j}$

Lemma 9.6 *Let $\boldsymbol{P} \in \mathbb{C}^{n\times n}$ be a projection matrix of rank 2 and $\boldsymbol{a}, \boldsymbol{b}, \boldsymbol{a}', \boldsymbol{b}' \in \mathbb{C}^n$, s.t. $\boldsymbol{a}^*\boldsymbol{b} = (\boldsymbol{a}')^*\boldsymbol{b}' = 1$, $\boldsymbol{a}'^*\boldsymbol{b} = \boldsymbol{a}^*\boldsymbol{b}' = \boldsymbol{b}^*\boldsymbol{b}' = 0$. If $\boldsymbol{P}(\boldsymbol{I}_n - \boldsymbol{a}\otimes\boldsymbol{b} - \boldsymbol{a}'\otimes\boldsymbol{b}') = \boldsymbol{0}$, then $\boldsymbol{P}$ is the projection of span$\{\boldsymbol{b}, \boldsymbol{b}'\}$.*

Proof Since

$$rank(\boldsymbol{I}_n) \le rank(\boldsymbol{I}_n - \boldsymbol{a}\otimes\boldsymbol{b} - \boldsymbol{a}'\otimes\boldsymbol{b}') + rank(\boldsymbol{a}\otimes\boldsymbol{b}) + rank(\boldsymbol{a}'\otimes\boldsymbol{b}'),$$

it follows that $rank(\boldsymbol{I}_n - \boldsymbol{a}\otimes\boldsymbol{b} - \boldsymbol{a}'\otimes\boldsymbol{b}') \ge n-2$. On the other hand, because $rank(\boldsymbol{P}) = 2$, $\boldsymbol{P}(\boldsymbol{I}_n - \boldsymbol{a}\otimes\boldsymbol{b} - \boldsymbol{a}'\otimes\boldsymbol{b}') = \boldsymbol{0}$ implies that $rank(\boldsymbol{I}_n - \boldsymbol{a}\otimes\boldsymbol{b} - \boldsymbol{a}'\otimes\boldsymbol{b}') \le n-2$. Hence $rank(\boldsymbol{I}_n - \boldsymbol{a}\otimes\boldsymbol{b} - \boldsymbol{a}'\otimes\boldsymbol{b}') = n-2$ and $\boldsymbol{P}$ is the projection of $col(\boldsymbol{I}_n - \boldsymbol{a}\otimes\boldsymbol{b} - \boldsymbol{a}'\otimes\boldsymbol{b}')^\perp$. On the other hand,

$$\begin{aligned}\boldsymbol{b}^*(\boldsymbol{I}_n - \boldsymbol{a}\otimes\boldsymbol{b} - \boldsymbol{a}'\otimes\boldsymbol{b}') &= \boldsymbol{b}^* - (\boldsymbol{b}^*\boldsymbol{a})\boldsymbol{b}^* - (\boldsymbol{b}^*\boldsymbol{a}')(\boldsymbol{b}')^* \\ &= \boldsymbol{b}^* - \boldsymbol{b}^* - 0\cdot(\boldsymbol{b}')^* = \boldsymbol{0}^*.\end{aligned}$$

Therefore, $\boldsymbol{P}\boldsymbol{b} = \boldsymbol{b}$. Similarly, $(\boldsymbol{b}')^*(\boldsymbol{I}_n - \boldsymbol{a}\otimes\boldsymbol{b} - \boldsymbol{a}'\otimes\boldsymbol{b}') = \boldsymbol{0}^*$ and $\boldsymbol{P}\boldsymbol{b}' = \boldsymbol{b}'$. Moreover, as $\boldsymbol{b}^*\boldsymbol{b}' = 0$ and $rank(\boldsymbol{P}) = 2$, $\boldsymbol{P} = \|\boldsymbol{b}\|^{-2}\cdot\boldsymbol{b}\otimes\boldsymbol{b} + \|\boldsymbol{b}'\|^{-2}\cdot\boldsymbol{b}'\otimes\boldsymbol{b}'$. □

Lemma 9.7 *Given $\widetilde{\mathbf{M}}[:, \widehat{0}](\boldsymbol{\omega})$ is full rank $\forall\boldsymbol{\omega}$, $\widetilde{\mathbf{M}}[\widehat{0}, :](\boldsymbol{\omega})$ is singular if (17) holds.*

Proof If (17) holds, then by Lemma 9.6, $\mathbf{m}_0^{\mathcal{E}}$, $\mathbf{m}_0^{\mathcal{O}}$ are orthogonal to $col(\widetilde{\mathbf{M}}[:, \widehat{0}])$, therefore $\left[\mathbf{m}_0^{\mathcal{O}}, \mathbf{m}_0^{\mathcal{E}}, \widetilde{\mathbf{M}}[:, \widehat{0}]\right] \in \mathbb{C}^{8\times 8}$ is full rank. Due to (17), $\mathbf{m}_0^{\mathcal{E}}$ and $\overline{\widetilde{\mathbf{m}_0}}^{\mathcal{E}}$ are not orthogonal to each other, hence $\left[\mathbf{m}_0^{\mathcal{O}}, \overline{\widetilde{\mathbf{m}_0}}^{\mathcal{E}}, \widetilde{\mathbf{M}}[:, \widehat{0}]\right] = \left[\mathbf{m}_0^{\mathcal{O}}, \widetilde{\mathbf{M}}\right]$

is full rank as well. Because $(\mathbf{m}_0^{\mathcal{O}})^*\widetilde{\mathbf{M}}[:, i] = 0,\ i = 0, \ldots, 7$ and $\mathbf{m}_0^{\mathcal{O}}[\widehat{0}]^*\widetilde{\mathbf{M}}[\widehat{0}, i] = (\mathbf{m}_0^{\mathcal{O}})^*\widetilde{\mathbf{M}}[:, i]$, $\mathbf{m}_0^{\mathcal{O}}[\widehat{0}]$ is orthogonal to $col(\widetilde{\mathbf{M}}[\widehat{0}, :])$. Since $\left[\mathbf{m}_0^{\mathcal{O}}[\widehat{0}], \widetilde{\mathbf{M}}[\widehat{0}, :]\right] \in \mathbb{C}^{7\times 8}$ is full rank, $\widetilde{\mathbf{M}}[\widehat{0}, :]$ must be singular. □

Proof of Proposition 5.3:

Proposition 5.3 Let $\widetilde{\mathbf{M}}[odd, \widehat{0}](\boldsymbol{\omega})$, $\widetilde{\mathbf{M}}[even, \widehat{0}](\boldsymbol{\omega}) \in \mathbb{C}^{4\times 6}$ be the submatrices of $\widetilde{\mathbf{M}}[:, \widehat{0}](\boldsymbol{\omega})$ consisting of odd and even indexed rows respectively. For any $\boldsymbol{\omega} \in S_0$, suppose (5.2.i) and (17) are satisfied, then (5.2.ii) holds if and only if $rank(\widetilde{\mathbf{M}}[odd, \widehat{0}](\boldsymbol{\omega})) = rank(\widetilde{\mathbf{M}}[even, \widehat{0}](\boldsymbol{\omega})) = 3$ and

$$[m_0(\boldsymbol{\omega}), m_0(\boldsymbol{\omega} + \boldsymbol{\pi}_2), m_0(\boldsymbol{\omega} + \boldsymbol{\pi}_4), m_0(\boldsymbol{\omega} + \boldsymbol{\pi}_6)]\, \widetilde{\mathbf{M}}[even, \widehat{0}](\boldsymbol{\omega}) = \mathbf{0}, \tag{28}$$

$$[m_0(\boldsymbol{\omega} + \boldsymbol{\pi}_1), m_0(\boldsymbol{\omega} + \boldsymbol{\pi}_3), m_0(\boldsymbol{\omega} + \boldsymbol{\pi}_5), m_0(\boldsymbol{\omega} + \boldsymbol{\pi}_7)]\, \widetilde{\mathbf{M}}[odd, \widehat{0}](\boldsymbol{\omega}) = \mathbf{0}. \tag{29}$$

Proof Note that $\widetilde{\mathbf{M}}[:, \widehat{0}]$ have the same rows at $\boldsymbol{\omega} + \boldsymbol{\pi}_i$, $i = 0, \ldots, 7$, we define row permutation matrix $\boldsymbol{P}_i,\ s.t.\ \boldsymbol{P}_i\left(\widetilde{\mathbf{M}}[:, \widehat{0}](\boldsymbol{\omega} + \boldsymbol{\pi}_i)\right) = \widetilde{\mathbf{M}}[:, \widehat{0}](\boldsymbol{\omega})$. Let $\boldsymbol{P}_{\widetilde{\mathbf{M}}}(\boldsymbol{\omega})$ be the projection matrix of the $col\left(\widetilde{\mathbf{M}}[:, \widehat{0}](\boldsymbol{\omega})\right)^{\perp} = null(\widetilde{\mathbf{M}}[:, \widehat{0}]^*)$, then (5.2.ii) is equivalent to $\boldsymbol{P}_{\widetilde{\mathbf{M}}}\boldsymbol{b}_0'(\boldsymbol{\omega}) = \mathbf{0}$. Group this equality at $\boldsymbol{\omega} + \boldsymbol{\pi}_i$, we have

$$\begin{aligned}
\mathbf{0} &= [\boldsymbol{P}_i \boldsymbol{P}_{\widetilde{\mathbf{M}}}\boldsymbol{b}_0'(\boldsymbol{\omega} + \boldsymbol{\pi}_i)]_{i=0,\ldots,7} \\
&= [\boldsymbol{P}_i \boldsymbol{P}_{\widetilde{\mathbf{M}}}(\boldsymbol{\omega} + \boldsymbol{\pi}_i)\boldsymbol{P}_i^2 \boldsymbol{b}_0'(\boldsymbol{\omega} + \boldsymbol{\pi}_i)]_{i=0,\ldots,7} \\
&= [\boldsymbol{P}_{\widetilde{\mathbf{M}}}(\boldsymbol{\omega})\boldsymbol{P}_i \boldsymbol{b}_0'(\boldsymbol{\omega} + \boldsymbol{\pi}_i)]_{i=0,\ldots,7} \\
&= \boldsymbol{P}_{\widetilde{\mathbf{M}}}(\boldsymbol{\omega})[\boldsymbol{P}_i \boldsymbol{b}_0'(\boldsymbol{\omega} + \boldsymbol{\pi}_i)]_{i=0,\ldots,7}
\end{aligned} \tag{41}$$

Let

$$\begin{aligned}
\overline{\widetilde{\mathbf{m}}_0}^{\mathcal{E}} &= [(1 + i \bmod 2) \cdot \overline{\widetilde{m}_0}(\boldsymbol{\omega} + \boldsymbol{\pi}_i)]_{i=0,\ldots,7}^{\top} = \widetilde{\mathbf{M}}[:, 0](\boldsymbol{\omega}), \\
\overline{\widetilde{\mathbf{m}}_0}^{\mathcal{O}} &= [(i \bmod 2) \cdot \overline{\widetilde{m}_0}(\boldsymbol{\omega} + \boldsymbol{\pi}_i)]_{i=0,\ldots,7}^{\top}, \\
\mathbf{m}_0^{\mathcal{E}} &= [(1 + i \bmod 2) \cdot m_0(\boldsymbol{\omega} + \boldsymbol{\pi}_i)]_{i=0,\ldots,7}^{\top}, \\
\mathbf{m}_0^{\mathcal{O}} &= [(i \bmod 2) \cdot m_0(\boldsymbol{\omega} + \boldsymbol{\pi}_i)]_{i=0,\ldots,7}^{\top}.
\end{aligned}$$

The identity constraint (17) thus can be written as $(\overline{\mathbf{m}_0^{\mathcal{E}}})^*\, \overline{\widetilde{\mathbf{m}}_0}^{\mathcal{E}} = 1$ and $(\overline{\mathbf{m}_0^{\mathcal{O}}})^*\, \overline{\widetilde{\mathbf{m}}_0}^{\mathcal{O}} = 1$. By definition,

$$\boldsymbol{P}_i \boldsymbol{b}_0'(\boldsymbol{\omega} + \boldsymbol{\pi}_i) = \boldsymbol{P}_i\left(\boldsymbol{b}_0 - m_0\widetilde{\mathbf{M}}[:, 0](\boldsymbol{\omega} + \boldsymbol{\pi}_i)\right) = \boldsymbol{b}_i - m_0(\boldsymbol{\omega} + \boldsymbol{\pi}_i)\boldsymbol{P}_i\left(\widetilde{\mathbf{M}}[:, 0](\boldsymbol{\omega} + \boldsymbol{\pi}_i)\right)$$

and

$$\boldsymbol{P}_i\left(\widetilde{\mathbf{M}}[:, 0](\boldsymbol{\omega} + \boldsymbol{\pi}_i)\right) = \begin{cases} \widetilde{\mathbf{M}}[:, 0] = \overline{\widetilde{\mathbf{m}}_0}^{\mathcal{E}}, & i \text{ is even} \\ \overline{\widetilde{\mathbf{m}}_0}^{\mathcal{O}}, & i \text{ is odd} \end{cases}$$

Substitute the above expression of $\boldsymbol{P}_i \boldsymbol{b}_0'(\boldsymbol{\omega}+\boldsymbol{\pi}_i)$ in (41) and we have

$$\mathbf{0} = \boldsymbol{P}_{\widetilde{\mathbf{M}}}(\boldsymbol{I}_8 - \overline{\widetilde{\mathbf{m}}_0}^{\mathcal{E}} \otimes \overline{\mathbf{m}_0^{\mathcal{E}}} - \overline{\widetilde{\mathbf{m}}_0}^{\mathcal{O}} \otimes \overline{\mathbf{m}_0^{\mathcal{O}}}) \tag{42}$$

Therefore, by Lemma 9.6, $\boldsymbol{P}_{\widetilde{\mathbf{M}}}$ is the projection of $span\{\overline{\mathbf{m}_0^{\mathcal{O}}}, \overline{\mathbf{m}_0^{\mathcal{E}}}\}$. This is equivalent to (28) and (29). Finally, since

$$6 = rank(\widetilde{\mathbf{M}}[:, \widehat{0}]) \le rank(\widetilde{\mathbf{M}}[odd, \widehat{0}]) + rank(\widetilde{\mathbf{M}}[even, \widehat{0}]) \le (4-1) + (4-1),$$

$$rank(\widetilde{\mathbf{M}}[odd, \widehat{0}]) = rank(\widetilde{\mathbf{M}}[even, \widehat{0}]) = 3.$$ □

Appendix 3: Joint Optimization of $c(\boldsymbol{\omega})$ and $\widetilde{m_0}(\boldsymbol{\omega})$

In Algorithm 1, $c(\boldsymbol{\omega})$ is chosen in step 3. to construct $m_0'(\boldsymbol{\omega})$, which replaces $m_0(\boldsymbol{\omega})$ and is used to create the linear constraint in (32) in step 4. Since different $c(\boldsymbol{\omega})$ correspond to different $m_0'(\boldsymbol{\omega})$, hence different linear constraints (31) on $\widetilde{m_0}(\boldsymbol{\omega})$; $\widetilde{m_0}(\boldsymbol{\omega})$ obtained in step 4. is optimal with respect to the pre-fixed $c(\boldsymbol{\omega})$ from step 3., but not necessarily global optimal considering all possible choices of $c(\boldsymbol{\omega})$. Therefore, we propose an alternative approach that combines step 3. and step 4. in Algorithm 1, where $c(\boldsymbol{\omega})$ and $\widetilde{m_0}(\boldsymbol{\omega})$ are jointly optimized to obtain $\widetilde{m_0}(\boldsymbol{\omega})$ with the best possible regularity given unregularized $m_0(\boldsymbol{\omega})$ from step 2.

By the definition in Proposition 5.4, $m_0'(\boldsymbol{\omega}) = m_0(\boldsymbol{\omega})c(\boldsymbol{\omega})$. Furthermore, since $c(\boldsymbol{\omega})$ is π-periodic in both $\omega_1,\ \omega_2$, we have $m_0'(\boldsymbol{\omega}+\boldsymbol{\pi}_i) = m_0(\boldsymbol{\omega}+\boldsymbol{\pi}_i)c(\boldsymbol{\omega}),\ i = 2, 4, 6$. Hence the constraint (17) on $\widetilde{m_0}(\boldsymbol{\omega})$ with $m_0(\boldsymbol{\omega})$ replaced by $m_0'(\boldsymbol{\omega})$ can be reformulated as follows,

$$\begin{aligned} 1 &= m_0'\widetilde{m_0}(\boldsymbol{\omega}) + m_0'\widetilde{m_0}(\boldsymbol{\omega}+\boldsymbol{\pi}_2) + m_0'\widetilde{m_0}(\boldsymbol{\omega}+\boldsymbol{\pi}_4) + m_0'\widetilde{m_0}(\boldsymbol{\omega}+\boldsymbol{\pi}_6) \\ &= c(\boldsymbol{\omega})\big(m_0\widetilde{m_0}(\boldsymbol{\omega}) + m_0\widetilde{m_0}(\boldsymbol{\omega}+\boldsymbol{\pi}_2) + m_0\widetilde{m_0}(\boldsymbol{\omega}+\boldsymbol{\pi}_4) + m_0\widetilde{m_0}(\boldsymbol{\omega}+\boldsymbol{\pi}_6)\big). \end{aligned} \tag{43}$$

Using the same setup of the optimization (32), we convert (43) to a constraint on a $2N \times 2N$ grid $\mathcal{G} = \{\boldsymbol{\omega}_i\}_{i=1}^{4N^2}$ of $[-\pi, \pi) \times [-\pi, \pi)$. Let $\widetilde{\mathbf{m}}_0 \in \mathbb{C}^{4N^2}$ and $\boldsymbol{A}_0 \in \mathbb{C}^{N^2 \times 4N^2}$ be the same as in (31) except that $\boldsymbol{A}_0$ is constructed by unregularized m_0 instead of m_0' for $\boldsymbol{A}$. Let $\boldsymbol{C} \in \mathbb{C}^{N^2 \times N^2}$ be a diagonal matrix whose j-th diagonal entry is $c(\boldsymbol{\omega}_j)$, where $\boldsymbol{\omega}_j \in \mathcal{G} \cap [-\pi, 0) \times [-\pi, 0)$ in the same order as the rows of $\boldsymbol{A}_0$. Then (43) is equivalent to the following constraint on the grid $\mathcal{G}$,

$$\boldsymbol{C}\boldsymbol{A}_0 \overline{\widetilde{\mathbf{m}}_0} = \mathbf{1}_{N^2}. \tag{44}$$

We formulate the joint optimization on $\boldsymbol{C}$ and $\widetilde{\mathbf{m}}_0$ analogous to (32) as follows,

$$\min_{\mathbf{x}\in\mathbb{C}^{4N^2},\ \mathbf{c}\in\mathbb{C}^{N^2}} \|\boldsymbol{D}\mathbf{x}\|^2, \quad s.t.\ \boldsymbol{C}\boldsymbol{A}_0\mathbf{x} = \mathbf{1},\ \boldsymbol{C} = diag(\mathbf{c}). \tag{45}$$

Since the objective function does not involve $\mathbf{c}$, $\mathbf{c}$ can be expressed in terms of $\mathbf{x}$ as long as $\boldsymbol{A}_0\,\mathbf{x}$ has no zero entry. Therefore, solving (43) is equivalent to solving the following optimization for $\widetilde{\mathbf{m}}_0$.

$$\min_{\mathbf{x}\in\mathbb{C}^{4N^2}} \|\boldsymbol{D}\mathbf{x}\|^2, \quad s.t.\ |\boldsymbol{A}_0\,\mathbf{x}| > 0, \tag{46}$$

where $|\cdot|$ in the constraint is a pointwise operator that computes the absolute value. The constraint $|\boldsymbol{A}_0\,\mathbf{x}| > 0$ can be rewritten as a set of quadratic constraints $\mathbf{x}^*\boldsymbol{Q}_i\mathbf{x} > 0,\ i = 0, \dots, N^2-1$ where $\boldsymbol{Q}_i = \boldsymbol{A}_0[i,:]^*\boldsymbol{A}_0[i,:]$. Therefore, (46) is a quadratically constrained quadratic program. Furthermore, since $\boldsymbol{Q}_i$ is positive semi-definite, (46) is not convex and is NP-hard in general. One may solve the convex relaxation of (46) using semidefinite programming (SDP). Instead of solving $\mathbf{x}$, we solve $\boldsymbol{X} \doteq \mathbf{x}\mathbf{x}^*$ and convert (46) into

$$\min_{\boldsymbol{X}\in\mathbb{C}^{4N^2\times 4N^2}} tr(\boldsymbol{D}^*\boldsymbol{D}\,\boldsymbol{X}), \quad s.t.\ tr(\boldsymbol{Q}_i\,\boldsymbol{X}) > 0,\ \boldsymbol{X}\succeq 0,\ rank(\boldsymbol{X}) = 1, \tag{47}$$

where $\boldsymbol{X}\succeq 0$ is the positive semidefinite constraint on $\boldsymbol{X}$. By removing the non-convex rank constraint $rank(\boldsymbol{X}) = 1$, (47) becomes a SDP and can be efficiently solved. Yet the solution $\boldsymbol{X}$ may not be rank 1 and require post processing (e.g. singular value decomposition) to obtain an approximate solution of (46).

Appendix 4: Supplementary Numerical Results

Numerical Optimization of $\widetilde{m_0}(\omega)$ in 1D

To test whether numerical optimization is a practical way to solve (17), we experiment on m_0 and $\widetilde{m_0}$ of existing real biorthogonal wavelets. We consider a pair of low frequency filters corresponding to biorthogonal scaling functions ϕ, $\tilde{\phi}$ with vanishing moments 3 and 5 respectively.

The 1D filters are shown in Fig. 12. Suppose we know the decomposition filter, and we want to find the real reconstruction filter, such that it has support as concentrated as possible. Figure 13 shows the ground truth m_0 and $\widetilde{m_0}$ considered in this simulation.

Let $\widehat{\widetilde{m_0}}(\boldsymbol{\omega})$ be the approximation of $\widetilde{m_0}(\boldsymbol{\omega})$, which is solution of the following optimization problem

$$\min_{\mathbf{x}} \|\boldsymbol{D}\mathbf{x}\|^2 + \|\mathbf{x}\|^2, \quad s.t.\ \boldsymbol{A}\mathbf{x} = \mathbf{1} \tag{48}$$

where $\boldsymbol{A}$ in the constraint is the matrix generated from $m_0\overline{\widetilde{m_0}}(\omega) + m_0\overline{\widetilde{m_0}}(\omega+\pi) = 1$, the 1D version of (17). Since only a single shift of π appears in the condition, each row of $\boldsymbol{A}$ has two non-zero entries. Figure 14 compares the solution of (48) and the ground truth. The support of the solution is slightly more spread out than the ground truth.

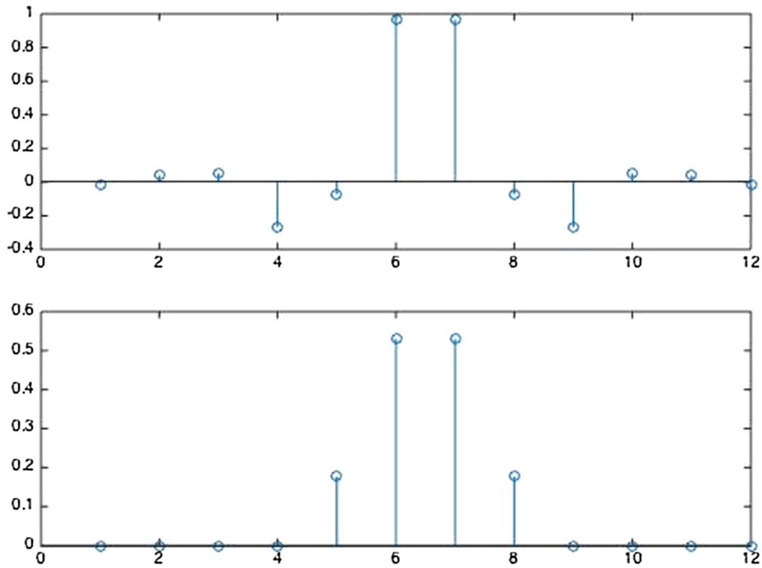

Fig. 12 1D filters, *up* LoD, *down* LoR

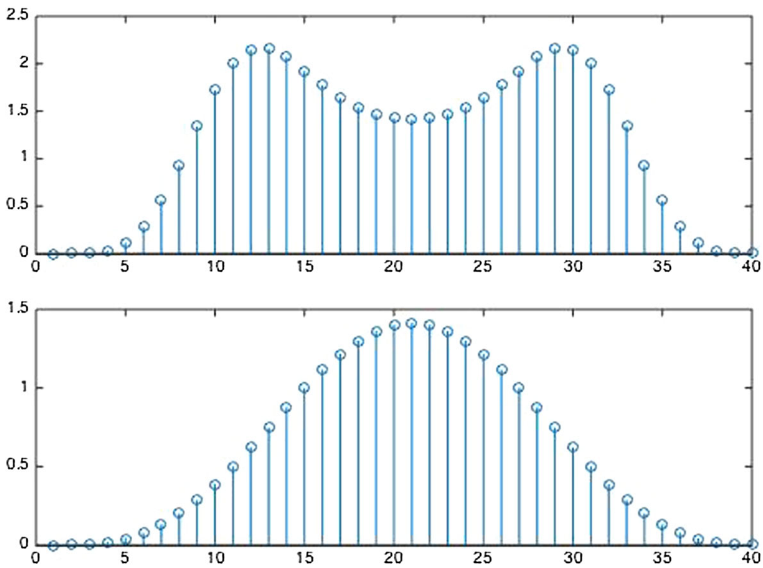

Fig. 13 $m_0(\omega)$ and $\widetilde{m_0}(\omega)$

Numerical Optimization of $\widetilde{m_0}(\omega)$ in 2D

In the 2D case, we use the pair of biorthogonal low-pass filters that are the tensor products of the 1D filters in Sect. 1 as ground truth. We solve the 2D version of the

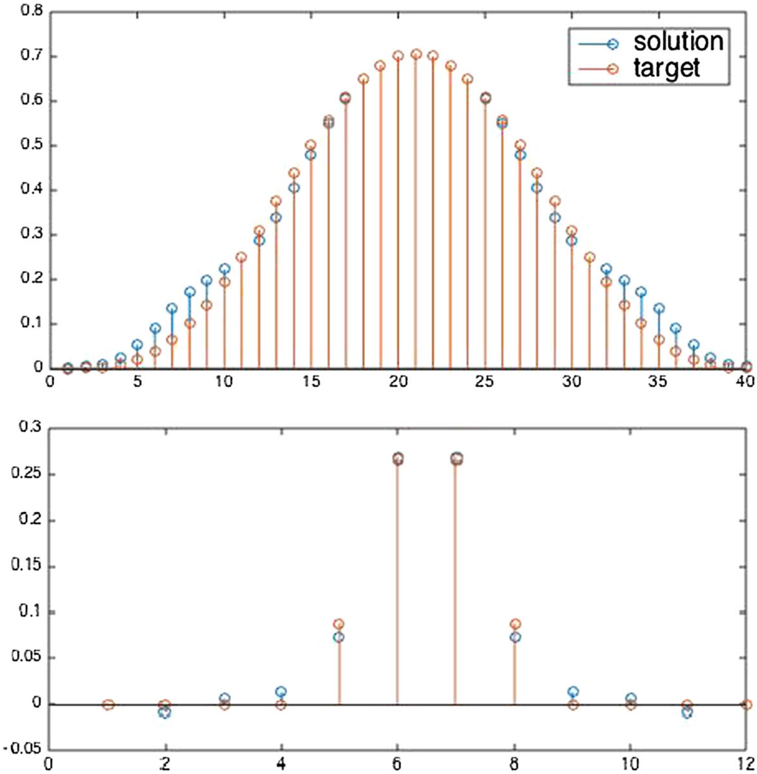

Fig. 14 $\widehat{\widetilde{m_0}}$ versus $\widetilde{m_0}$, *top* frequency domain, *bottom* time domain

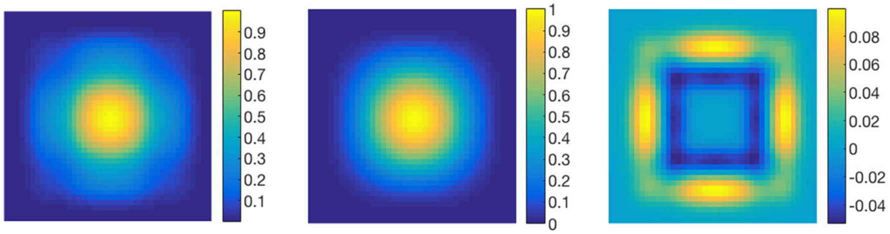

Fig. 15 *Left to right* solution of (48) in 2D, ground truth and their difference

optimization problem (48). Figure 15 shows the solution and compares it with the ground truth.

To make the support of $\widehat{\widetilde{m_0}}(\boldsymbol{\omega})$ better concentrate within the low frequency domain, we change the squared ℓ_2-norm penalty in (48) to a weighted version (corresponding to Modulation space) as follows,

$$\min_{\mathbf{x}} \ \|\boldsymbol{D}\mathbf{x}\|^2 + \lambda \|\mathbf{w} \circ \mathbf{x}\|^2, \quad s.t. \ \boldsymbol{A}\mathbf{x} = \mathbf{1} \tag{49}$$

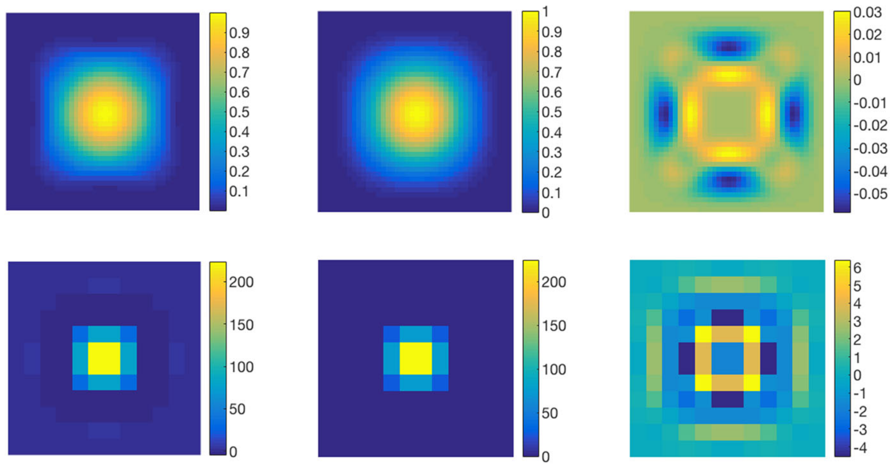

Fig. 16 *Left to right* solution of (49) ($\lambda = 600$), ground truth and their difference; *Top* frequency domain, *bottom* time domain

where $\circ$ is Hadamard product and $\mathbf{w}$ is a weight vector. In particular, we choose $\forall \boldsymbol{\omega},\ \mathbf{w}(\boldsymbol{\omega}) = |\boldsymbol{\omega}|$. Figure 16 shows the solution of (49) with $\lambda = 600$.

Compared to (32) proposed to solve $\widetilde{m_0}(\boldsymbol{\omega})$, both optimization problems (48) and (49) in this simulation minimize the squared ℓ_2-norm of the gradient of $\widetilde{m_0}$ but have an extra (weighted) ℓ_2 regularization term. Although (48) and (49) work better than (32) for 1D and 2D tensor wavelet construction here, they do not provide solutions with better regularity in the construction of biorthogonal directional wavelets while increasing the computation cost.

References

1. Bamberger, R.H., Smith, M.J.T.: A filter bank for the directional decomposition of images: theory and design. IEEE Trans. Signal Process. **40**(4), 882–893 (1992)
2. Blanchard, J., Krishtal, I.: Matricial filters and crystallographic composite dilation wavelets. Math. Comput. **81**(278), 905–922 (2012)
3. Candes, E., Demanet, L., Donoho, D., Ying, L.: Fast discrete curvelet transforms. Multiscale Model. Simul. **5**(3), 861–899 (2006)
4. Cohen, A., Daubechies, I., Feauveau, J.-C.: Biorthogonal bases of compactly supported wavelets. Commun. Pure Appl. Math. **45**(5), 485–560 (1992)
5. Cohen, A., Schlenker, J.-M.: Compactly supported bidimensional wavelet bases with hexagonal symmetry. Constr. Approx. **9**(2–3), 209–236 (1993)
6. Do, M.N., Vetterli, M.: The contourlet transform: an efficient directional multiresolution image representation. IEEE Trans. Image Process. **14**(12), 2091–2106 (2005)
7. Durand, S.: M-band filtering and nonredundant directional wavelets. Appl. Comput. Harmon. Anal. **22**(1), 124–139 (2007)
8. Easley, G.R., Labate, D.: Critically sampled composite wavelets. In: Proceedings of the 2009 Conference Record of the Forty-Third Asilomar Conference on Signals, Systems and Computers, pp. 447–451. IEEE (2009)
9. Easley, G., Labate, D., Lim, W.-Q.: Sparse directional image representations using the discrete shearlet transform. Appl. Comput. Harmon. Anal. **25**(1), 25–46 (2008)

10. Goossens, B, Aelterman, J, Luong, H., Pižurica, A., Philips, W.: Design of a tight frame of 2d shearlets based on a fast non-iterative analysis and synthesis algorithm. SPIE Optics and Photonics, pp. 81381Q (2011)
11. Han, B., Zhao, Z., Zhuang, X.: Directional tensor product complex tight framelets with low redundancy. Appl. Comput. Harmon. Anal. **41**(2), 603–637 (2016)
12. Kutyniok, G., Lim, W.-Q., Zhuang, X.: Digital shearlet transforms. In: Shearlets, pp. 239–282. Springer, Berlin (2012)
13. Nguyen, T.T., Oraintara, S.: Multiresolution direction filterbanks: theory, design, and applications. IEEE Trans. Signal Process. **53**(10), 3895–3905 (2005)
14. Sauer, T.: Shearlet multiresolution and multiple refinement. In: Kutyniok, G. (ed.) Shearlets. Multiscale Analysis for Multivariate Data, pp. 199–237. Applied and Numerical Harmonic Analysis, Birkhäuser (2012)
15. Selesnick, I.W., Baraniuk, R.G., Kingsbury, N.C.: The dual-tree complex wavelet transform. IEEE Signal Process. Mag. **22**(6), 123–151 (2005)
16. Yin, R.: Construction of orthonormal directional wavelets based on quincunx dilation subsampling. In: Proceedings of the 2015 International Conference on Sampling Theory and Applications (SampTA), May 2015, pp. 292–296 (2015)